Sedimentology (2013) doi: 10.1111/sed.12033

Techniques for assessing spatial heterogeneity of carbonate $\delta^{13}C$ values: Implications for craton-wide isotope gradients

J. GARRECHT METZGER and DAVID A. FIKE
Department of Earth and Planetary Sciences, Washington University, St. Louis, MO 63130, USA (E-mail: gmetzger@levee.wustl.edu)

Associate Editor – Adrian Immenhauser

ABSTRACT

The sedimentary record of carbonate carbon isotopes ($\delta^{13}C_{carb}$) provides one of the best methods for correlating marine strata and understanding the long-term evolution of the global carbon cycle. This work focuses on the Late Ordovician Guttenberg isotopic carbon excursion, a *ca* 2·5‰ positive $\delta^{13}C_{carb}$ excursion that is found in strata globally. Substantial variability in the apparent magnitude and stratigraphic morphology of the Guttenberg excursion at different localities has hampered high-resolution correlations and led to divergent reconstructions of ocean chemistry and the biogeochemical carbon cycle. This work investigates the magnitude, spatial scale and sources of isotopic variability of the Guttenberg excursion in two sections from Missouri, USA. Centimetre-scale isotope transects revealed variations in $\delta^{13}C_{carb}$ and $\delta^{18}O_{carb}$ greater than 2‰ across individual beds. Linear $\delta^{13}C_{carb}$ to $\delta^{18}O_{carb}$ mixing lines, together with petrographic and elemental abundance data, demonstrate that much of the isotopic scatter in single beds is due to mixing of isotopically distinct components. These patterns facilitated objective sample screening to determine the 'least-altered' data. A $\delta^{18}O_{carb}$ filter based on empirical $\delta^{18}O_{carb}$ values of well-preserved carbonate mudstones allowed further sample discrimination. The resulting 'least-altered' $\delta^{13}C_{carb}$ profile improves the understanding of regional as well as continental-scale stratigraphic relations in this interval. Correlations with other Laurentian sections strongly suggest that: (i) small-scale variability in Guttenberg excursion $\delta^{13}C_{carb}$ values may result in part from local diagenetic overprinting; (ii) peak-Guttenberg excursion $\delta^{13}C_{carb}$ values of the Midcontinent are not distinct from their Taconic equivalents; and (iii) no primary continental-scale spatial gradient in $\delta^{13}C_{carb}$ (for example, arising from chemically distinct 'aquafacies') is required during Guttenberg excursion-time. This study demonstrates the importance of detailed petrographic and geochemical screening of samples to be used for $\delta^{13}C_{carb}$ chemostratigraphy and for enhancing understanding of epeiric ocean chemistry.

Keywords Aquafacies, carbonate diagenesis, chemostratigraphy, Guttenberg excursion, isotope gradients, isotopic heterogeneity, sea water aging, sedimentation rate.

INTRODUCTION

General background

Secular variation in the carbon isotopic composition of marine limestones can be used to map the spatial and temporal patterns in sedimentation across basins and to link these to environmental and ecological changes. A time-varying $\delta^{13}C$ signal in the marine dissolved inorganic carbon (DIC) reservoir can arise from changes in the flux and isotopic composition of the major sources

and sinks of carbon to and from the ocean (Kump & Arthur, 1999). The variation in $\delta^{13}C_{DIC}$ can be captured in coeval sediment as carbonate carbon ($\delta^{13}C_{carb}$) or following biological uptake as organic carbon ($\delta^{13}C_{org}$). The resulting $\delta^{13}C$ data provide a means to correlate sedimentary strata within and between sedimentary basins by aligning their $\delta^{13}C$ chemostratigraphic profiles (e.g. Knoll *et al.*, 1986; Hayes *et al.*, 1999) revealing stratigraphic information undetectable using conventional lithostratigraphic or biostratigraphic methods. For example, discontinuous changes in $\delta^{13}C_{carb}$ profiles provide a means to identify cryptic hiatal surfaces in sedimentary strata (e.g. Jones *et al.*, 2011) because $\delta^{13}C_{carb}$ should smoothly vary when deposition is continuous. Even when deposition is continuous, various post-depositional processes, such as microbial oxidation of organic carbon (Patterson & Walter, 1994) and meteoric diagenesis (Allan & Matthews, 1982; Joachimski, 1994; Immenhauser *et al.*, 2002), may alter a primary $\delta^{13}C_{carb}$ signal, typically toward more ^{13}C-depleted values. As such, screening for diagenetic alteration is critical when using $\delta^{13}C_{carb}$ data for basinal correlation or for reconstructing the evolution of the global carbon cycle.

The potential utility of $\delta^{13}C_{carb}$ chemostratigraphy for correlations and environmental reconstructions depends on spatial homogeneity in the isotopic composition of the marine DIC reservoir. Recently, it has been suggested that many marine strata, particularly those formed in epeiric settings with uncertain connections to the global ocean, have carbon isotope signatures in which local processes (for example, aging of the water mass; Immenhauser *et al.*, 2008) variably overprint a global $\delta^{13}C$ signal (Simo *et al.*, 2003; Panchuk *et al.*, 2005, 2006; Fanton & Holmden, 2007; Brand *et al.*, 2009), complicating regional-scale to global-scale correlations and attempts to understand the processes driving carbon cycle variability.

This work focuses on the Guttenberg carbon isotope excursion, a positive *ca* 2·5‰ excursion in $\delta^{13}C_{carb}$ during the Mohawkian Series of the Upper Ordovician, which provides an example where chemostratigraphy has allowed for regional and global correlation of strata from different palaeoenvironments across much of the United States (Patzkowsky *et al.*, 1997; Ludvigson *et al.*, 2000, 2004; Young *et al.*, 2005; Bergström *et al.*, 2010a,b; Coates *et al.*, 2010), portions of southeastern Canada (Bergström *et al.*, 2010a,b), Sweden (Bergström *et al.*, 2004), Estonia (Martma, 2005; Kaljo *et al.*, 2007), China (Young *et al.*, 2005; Bergström *et al.*, 2009a) and Malaysia (Bergström *et al.*, 2010c). However, differences in the stratrigraphic expression of the Guttenberg excursion (including the shape of the $\delta^{13}C_{carb}$ curve as a function of stratigraphic position, as well as the pre-excursion, peak-excursion and post-excursion $\delta^{13}C_{carb}$ values and the degree of scatter) have hampered detailed correlation between sections and obscured a fundamental understanding of the environmental and/or ecological changes that caused the Guttenberg excursion (Patzkowsky *et al.*, 1997; Ludvigson *et al.*, 2004; Panchuk *et al.*, 2005, 2006; Young *et al.*, 2005, 2008; Bergström *et al.*, 2010a).

In North America, stratigraphic correlations have been facilitated by the co-occurrence of the Guttenberg excursion and the two widely traceable K-bentonites, the Deicke and Millbrig (Kolata *et al.*, 1986, 1987, 1996, 1998, 2001). These bentonites act as time markers used to test chemostratigraphic and sequence stratigraphic models, providing a framework in which to investigate temporal and spatial variation in sedimentation rates (Leslie & Bergström, 1997), erosion (Railsback *et al.*, 2003), facies migration and sequence development (Holland & Patzkowsky, 1998), as well as geochemical and isotopic heterogeneities in carbonates and their palaeoceanographic sources (Panchuk *et al.*, 2006; Fanton & Holmden, 2007). Ordovician strata are replete with bentonites (e.g. Kolata *et al.*, 1996) and care must be taken in cross-continental correlation of K-bentonites, as apatite phenocryst geochemistry (Sell & Samson, 2011) and radiometric ages (e.g. Huff, 2008) of Laurentian and Baltoscandian K-bentonites suggest that some previous bentonite-based correlations may not be correct.

The goals of this work are to: (i) document cm-scale variability in $\delta^{13}C_{carb}$ and $\delta^{18}O_{carb}$ and use petrographic and trace geochemical indicators of diagenesis to understand the processes by which isotopic signals can be altered as they relate to depositional setting; (ii) develop an objective sample screening procedure to be used in bulk carbonate analysis for identifying least-altered data; (iii) use $\delta^{13}C_{carb}$ chemostratigraphy to correlate between two localities in Missouri, USA and re-evaluate existing stratigraphic relations; and (iv) use this interpretative framework to compare the stratigraphic expression of the Guttenberg excursion in Missouri with existing records from across the continent to test hypotheses on the existence of large-scale (10^3 to

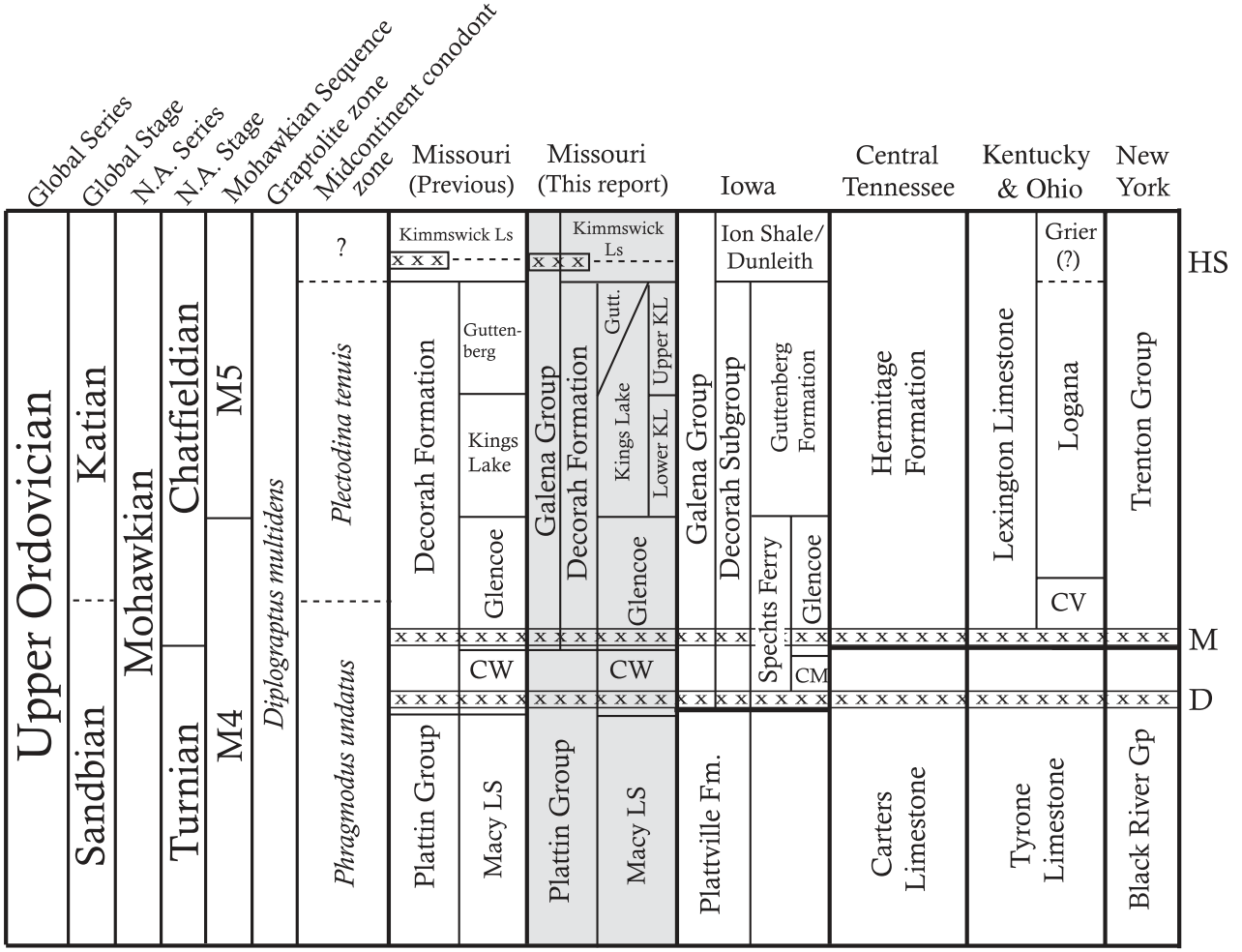

Fig. 1. Proposed chronostratigraphic relations of select locations within the United States. Series and stages taken from Bergström *et al.* (2009b). M4 and M5 refer to Mohawkian sequences (Holland & Patzkowsky, 1997, 1998). Biozones taken from Leslie (2000). Information for 'Missouri (previous)' taken from Thompson (1991). 'Missouri (this report)' constructed from new data and placement of the Castlewood Limestone into the Plattin group according to Kolata *et al.* (1998). 'Upper KL' and 'Lower KL' correspond to new divisions of the Kings Lake Limestone used in this work for central-southern Missouri. Iowa stratigraphy adapted from Ludvigson *et al.* (2004). Kentucky and Ohio information taken from Leslie (2000) and McLaughlin & Brett (2007). New York information adapted from Leslie (2000) and Mitchell *et al.* (2004). Horizontal bars with 'X' correspond to K-bentonites. CM = Carimona, CV = Curdsville, CW = Castlewood, D = Deicke K-bentonite, Fm = Formation, Gp = Group, HS = House Springs K-bentonite, KW = Kimmswick Limestone, Ls = Limestone, M = Millbrig K-bentonite. Where correlations are ambiguous dashed lines and question marks are used.

10^4 km) spatial gradients in $\delta^{13}C_{carb}$ (i.e. 'aquafacies' of Holmden *et al.*, 1998) at this time.

Geological setting

Strata investigated in the present study occur within the Mohawkian Series of North America, which is roughly equivalent to the uppermost Sandbian to lower Katian Global Series (Fig. 1; Bergström *et al.*, 2009b). Sections begin in the uppermost Turinian and end in the lower to middle Chatfieldian (North American Stages) based on correlations using globally extensive K-bentonites and biostratigraphy (Thompson, 1991; Leslie, 2000; Bergström *et al.*, 2009b, 2010a,b). During this time, Missouri was located in sub-equatorial latitudes 15 to 30°S (Scotese & McKerrow, 1990) where sedimentation occurred in a warm, shallow sea (Fig. 2A). The Mohawkian contains a major change in sediment deposition across Missouri (Thompson, 1991), other portions of the upper Mississippi Valley (Kolata *et al.*, 1998) and the mid-South (Holland & Patzkowsky, 1998). In Missouri, the geographic thickness patterns of stratigraphic units become roughly inverted by early Chatfieldian time

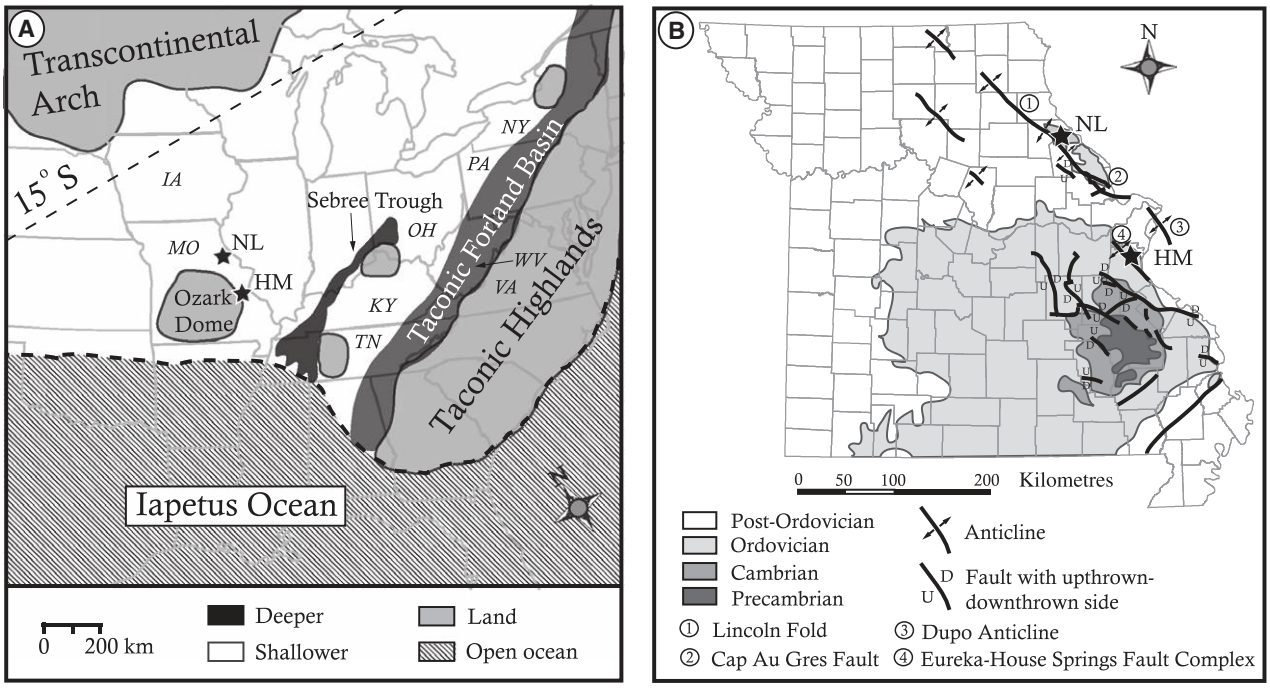

Fig. 2. (A) Palaeogeographic map showing general depositional environment and important geological structures (adapted from Scotese & McKerrow, 1990; Holland & Patzkowsky, 1998; Kolata *et al.*, 2001; Simo *et al.*, 2003). Stars represent sample locations HM = Highway MM and NL = New London. State abbreviations (italics) are as follows: IA = Iowa, KY = Kentucky, MO = Missouri, NY = New York, OH = Ohio, PA = Pennsylvania, TN = Tennessee, VA = Virginia and WV = West Virginia. (B) Map of Missouri showing sample locations, generalized surface stratigraphy (under the Pleistocene alluvium) and major structural features of eastern Missouri. Surface strata adapted from Missouri Department of Natural Resources (2009). Structural features adapted from McCracken (1966). Strata are sedimentary except Precambrian igneous rocks.

(Kolata *et al.*, 1998) as the carbonate depocentre shifted north towards Iowa. The uplift of the Ozark Dome (modern day St. Francois Mountains) may have partially controlled sedimentation patterns and is thought to have intermittently interrupted regional carbonate sedimentation during the Early to Middle Ordovician, although sedimentation became more continuous during the Late Ordovician highstand (McCracken, 1966; Thompson, 1991). Further, the rhyolites and granites of the Ozark dome may have been an important siliciclastic source for the present study sections (Fig. 2B). Although Mohawkian-aged strata in Missouri have been studied for over 100 years (e.g. Ulrch, 1904; Kay, 1935; Templeton & Willman, 1963; Kolata *et al.*, 1986), there is a dearth of literature that directly focuses on their deposition, sequence stratigraphy and chemostratigraphy, especially when compared to the time-equivalent Trenton-Black River succession of the eastern United States (e.g. Brett *et al.*, 2004; Mitchell *et al.*, 2004; McLaughlin & Brett, 2007).

Chronostratigraphic relations of selected Upper Ordovician sections across the North American Craton are shown in Fig. 1 and were constructed using K-bentonite stratigraphy, biostratigraphy and $\delta^{13}C_{carb}$ stratigraphy. The studied interval ranges from the upper Plattin Group through the lower Kimmswick Limestone. The Plattin Group (Platteville equivalent outside of Missouri, Fig. 1) is thickest in nearby south-western Illinois where it reaches over 200 m (Kolata *et al.*, 2001). The Plattin is *ca* 140 m thick in south-eastern Missouri near Cape Girardeau and thins north-westward, where 300 km north-west it is 14 m thick (Martin *et al.*, 1961). The Plattin is uppermost Turinian and is equivalent to the upper Black River succession of New York, based on K-bentonite stratigraphy of the Deicke K-bentonite dated to 454·5 ± 0·5 Ma (Tucker, 1992) and conodont biostratigraphy (Leslie, 2000; Brett *et al.*, 2004). The Plattin Group is interpreted to represent a major transgressive cycle as flooding spread north and west from the Sebree Trough, a bathymetric low that runs north-east to south-west along the north-western Kentucky border (Witzke & Kolata, 1988). Plattin Group strata are dominated by thin-bedded, somewhat nodular mudstones

characterized by fine-grained, heavily bioturbated, high-purity (>95% carbonate) limestones with partially dolomitized burrows (Thompson, 1991).

The overlying Galena Group is thickest in the north-west and pinches out approaching the Sebree Trough, where Plattin Group deposits are thickest; this represents an apparent restructuring of sediment deposition patterns from Plattin time (Witzke & Kolata, 1988). In Missouri, Galena Group strata comprise the Decorah Formation (composed of the Glencoe Shale, Kings Lake Limestone and Guttenberg Limestone) and the overlying Kimmswick Limestone. The Glencoe Shale contains dark, thinly bedded, fissile, carbonate-poor shales intercalated with planar, thin, sometimes discontinuous brachiopod-bryozoan calcarenites and calcirudites (Thompson, 1991; Kolata *et al.*, 1998), as well as the Millbrig K-bentonite, which is dated to 453·1 ± 1·3 Ma (Tucker & McKerrow, 1995) and defines the Turinian-Chatfieldian boundary (Ludvigson *et al.*, 2004). The overlying Kings Lake Limestone is composed mostly of blue-grey carbonate mudstones and storm-bed packstones, both with thin blue shale partings. Kings Lake facies have been interpreted as transitional between the Glencoe Shale and the overlying Guttenberg Limestone in north-eastern Missouri (Kolata *et al.*, 1986). In central and southern Missouri, the Kings Lake Limestone is unconformably overlain by the Kimmswick Limestone, while it is conformable with the overlying Guttenberg Limestone in northernmost Missouri. The Guttenberg Limestone is only found north of St. Louis, Missouri and like the underlying Kings Lake Limestone, is composed of mudstones with frequent carbonate storm beds. In Missouri, the brown mud and shale partings of the Guttenberg distinguish the unit from the underlying blue-grey mud and shale partings of the Kings Lake Limestone. The contact between the Decorah Formation and the overlying Kimmswick Limestone is a minor unconformity with rip-up lithoclasts from the Guttenberg Limestone (northern Missouri) and Kings Lake Limestone (southern Missouri) found in the lowermost 20 cm of the Kimmswick Limestone (Kolata *et al.*, 1998).

The Kimmswick Limestone is a well-cemented, medium to fine-grained crinoid-brachiopod-bryozoan grainstone (Thompson, 1991; Kolata *et al.*, 1998). Strata are thick to massively bedded with evidence for crossbedding rare or absent in upper portions (Thompson, 1991). The Kimmswick is a very pure limestone (>98% carbonate) that contains abundant centimetre diameter burrows that weather to a 'Swiss-cheese' texture similar to the Plattin Limestone. It is exposed at the surface in northern Missouri and erosionally truncated and overlain by Mid–Late Paleozoic sandstones south of St. Louis.

Study locations

Two locations in eastern Missouri were chosen for high-resolution chemostratigraphic study (Fig. 2). The first site is located 8 km south of New London, Missouri along the eastern frontage road (East Side Drive) off of Highway 61, which is located a few hundred m north of Spencer Creek (Latitude: 39·522415°N; Longitude: 91·344629°W). The New London section is the same as Location 53 in Kolata *et al.* (1986). The sampled interval begins with 7·5 m of the upper Plattin Limestone and continues through the Decorah Formation and extends 8 m into the Kimmswick Limestone (Fig. 3). The second site, Highway MM, is a fresh road-cut exposure found along Missouri State Highway MM near Barnhart, Missouri (Latitude: 38·394101°N, Longitude: 90·543364°W) approximately 15 km west of Location 63 of Kolata *et al.* (1986). This study is the first published geological record for this location that the authors are aware of. The Highway MM section begins in the uppermost 10 to 15 m of the Plattin Limestone and continues through the Decorah Formation and into the first 5 m of the Kimmswick Limestone (Fig. 4).

METHODS

Sampling and petrology

Field sampling in both locations was completed over a lateral distance of *ca* 300 m along a single outcrop face. Individual beds (Highway MM: $n = 80$; New London: $n = 69$) were sampled at regular intervals where possible and some beds were collected in replicate (Tables S1 and S2). No large faults, fractures, folds, joints, or igneous features were observed at either location. Stratigraphic columns were constructed using a combination of the Dunham nomenclature and Wentworth-Udden grain-size terminology (Flügel, 2009). Stratigraphic units were identified in the field using the criteria in Thompson (1991). Deicke, Millbrig and House Springs K-bentonites were identified in the field based on stratigraphic position (Kolata *et al.*, 1986),

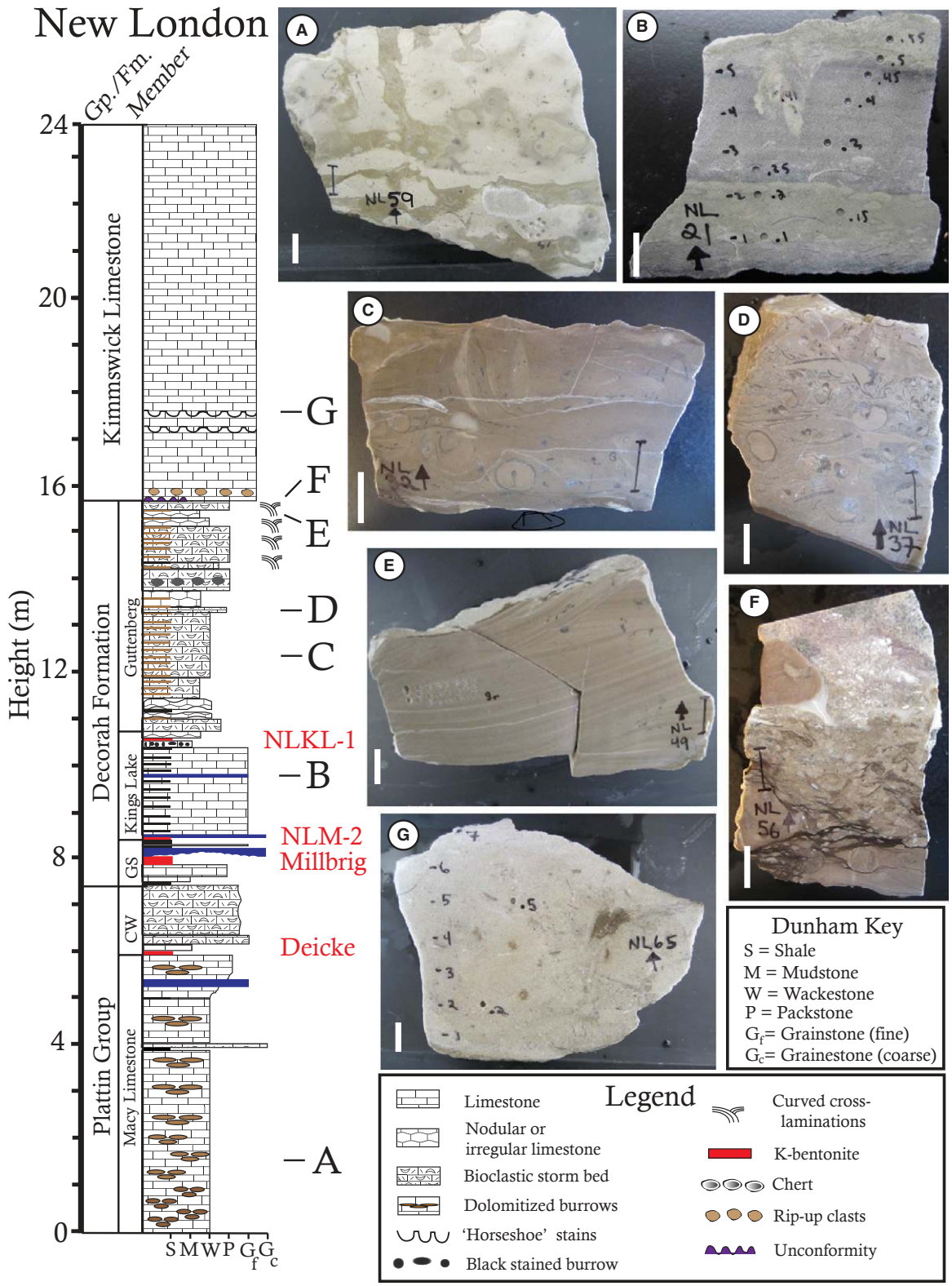

Fig. 3. Lithology and selected facies for New London. See Fig. 1 for biozone, sequence and stratigraphic designations. Scale bars (white) are 1 cm. Pen markings used for carbonate sampling. Samples are as follows: (A) NL59, lower Plattin wackestone; (B) NL21, burrowed calcarenite with dolomitic zones (green); (C) NL32, muddy tempestite wackestone; (D) NL37, muddy tempestite packstone; (E) NL49, cross-laminated mudstone; (F) NL56, lowermost Kimmswick with Guttenberg rip-up clasts; (G) NL65, clean Kimmswick grainstone with burrowing (brown).

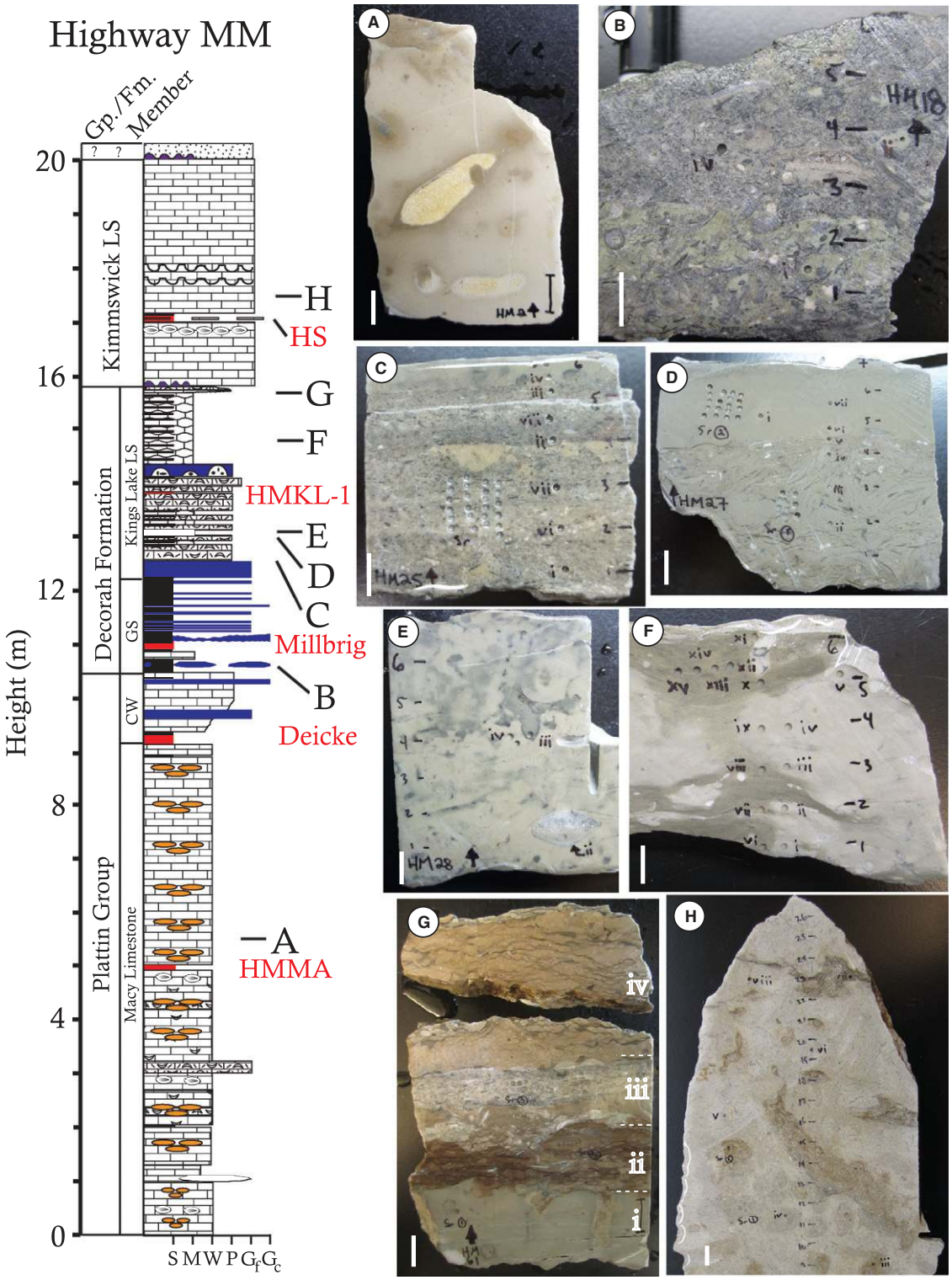

Fig. 4. Lithology and selected facies for Highway MM. See Fig. 1 for biozone, sequence and stratigraphic designations. See Fig. 3 for legend. Scale bars (white) are 1 cm. Pen markings used for carbonate sampling. Samples are as follows: (A) HM2, upper Plattin mudstone-wackestone with yellow dolomitized burrows; (B) HM18, coarse-grained calcarenite with dolomitic green clay; (C) HM25, fine-grained calcarenite; (D) HM27, tempestite packstone; (E) HM28, mudstone with black stained burrows; (F) HM55, wackestone showing dolomitic 'wispy brushtrokes'; (G) HM61, zone i (0 to 3 cm) mudstone capped by hardground, zone ii (3 to 5 cm) is argillaceous and dolomitized, zone iii (5 to 8 cm) is a tempestite lens and zone iv (8 to 14 cm) is stylonodular mudstone; (H) HM42, burrowed lower Kimmswick grainstone.

thickness, colour, clay content, degree of lithification, bedding geometry and zircon abundance. In addition, several minor bentonites (HMMA, HMKL-1, NLKL-1 and NLM-2) were identified and named for the location/formation. Two of these bentonites (HMKL-1 and NLKL-1) were tentatively correlated in this study and may be equivalent to the Elkport K-bentonite of the upper Mississippi Valley (Kolata *et al.*, 1986); however, no definitive correlation of these minor bentonites to equivalents outside of the study area is made.

Forty-seven thin sections from 45 individual beds were analysed under transmitted and reflected light microscopy on a Leica petrographic microscope (model DM-2500P; Leica Microsystems GmbH, Wetzlar, Germany) with a maximum magnification of 500×. Photographs were taken with a Leica (model DFC 295) microscope-mounted camera.

Geochemical methods

Stable carbon and oxygen isotope analysis of carbonate

Carbonate samples were drilled from polished rock slabs cut perpendicular to the bedding plane using a Woodtek Drill (model 109370; Woodworkers Supply Inc., Casper, Wyoming, USA) fitted with 1 to 2 mm carbide drill bit tips. Powdered samples were placed in vials, flushed with He gas, and converted to CO_2 through reaction with anhydrous phosphoric acid (Epstein & Mayeda, 1953). Acidified samples were heated for 1 to 23 h at 70°C on a Gas Bench II (Thermo Fisher Scientific, Waltham, MA, USA). Evolved CO_2 was analysed on a Thermo Fischer Delta V Plus Isotope Ratio Mass Spectrometer at Washington University. Values are reported in per mil (‰) relative to the Vienna Pee Dee belemnite (VPDB) standard. All runs contained internal standards as well as international standards NBS-18, NBS-19 and LSVEC. For a single run, one standard deviation (1σ) averaged 0·04‰ for $\delta^{13}C_{carb}$ and $\delta^{18}O_{carb}$ for all standards, while average reproducibility (1σ) for $\delta^{13}C_{carb}$ of replicate samples for a single run was 0·07‰. Reproducibility (1σ) across all sampling days for $\delta^{13}C_{carb}$ was 0·09‰ for NBS-18, 0·10‰ for NBS-19 and 0·25‰ for LSVEC, and for $\delta^{18}O_{carb}$ was 0·12‰ for NBS-18 and NBS-19 and 0·13‰ for LSVEC.

Samples were dominantly micrite and skeletal grainstones with no large altered phases or features (for example, spar, marl, stylolites, dolomitized burrows, etc.), although selected diagenetic textures were analysed to test for isotopic alteration and trace element abundance patterns as a function of distance from the altered texture. The desired sampling resolution in these sections precluded relying on a brachiopod-based approach (Veizer *et al.*, 1997, 1999; Brand, 2004). In total, more than 700

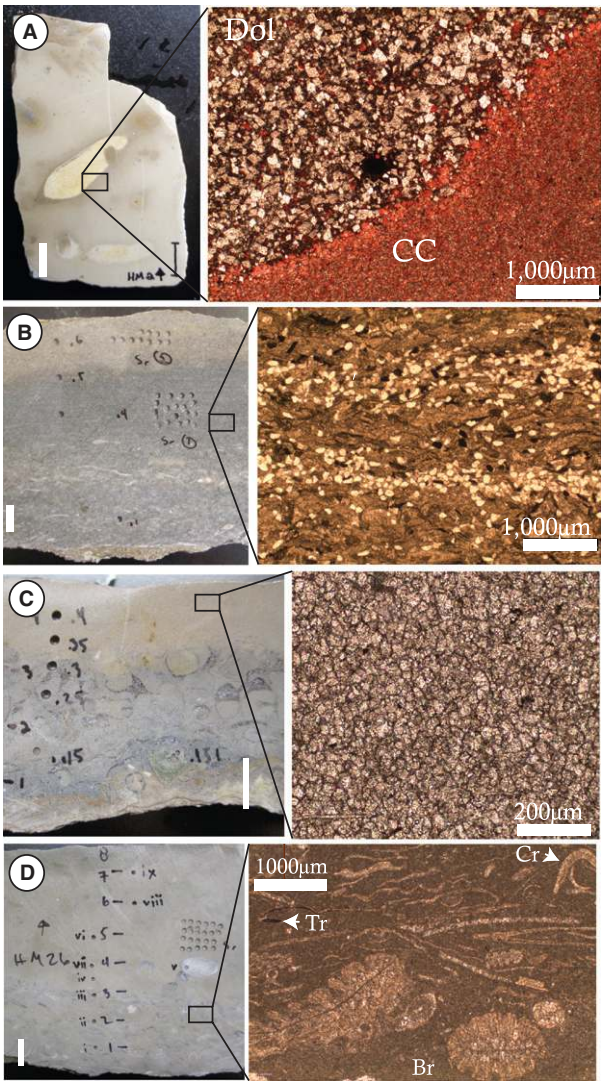

Fig. 5. Thin section photomicrographs and their corresponding hand sample location. Scale bars in hand samples (white) are 1 cm. (A) Stained thin section of HM2 in plane polarized light shows muddy and dolomitized burrows. Calcite (CC) is red and dolomite (Dol) is white. Darker spots in hand sample are dolomitized similar to yellow burrows. (B) Fine-grained calcarenite NL19 in plane polarized light. (C) NL14 under plane-polarized light showing carbonate silt or mud aggregates that possibly formed by vadose zone alteration. (D) HM26 with plane-polarized light shows whole bioclast-bearing storm bed. Tr = trilobite (partially pyritized), Cr = crinoid arm and Br = bryozoan

samples (with over 100 duplicates) were drilled with multiple parallel transects to identify lateral intra-sample variability and pinpoint the mixing of isotopically distinct components. More than 450 samples were screened to construct bed-averaged isotope values for 66 beds from Highway MM and 69 beds from New London. Bed-averaged values were obtained by taking an unweighted average of individual microdrilled samples identified as 'least-altered' based on textural and petrographic analyses (see below).

Carbonate content (%carb), total organic carbon content (TOC), $\delta^{13}C_{org}$

Weight percent carbonate (wt% $CaCO_3$) was determined using a gravimetric method from the dissolution of 2 to 5 g of bulk material. Hand samples were cut in 2 cm vertical intervals to document vertical variability across a single bed. Diagenetic textures were avoided. Total organic carbon content (TOC) and $\delta^{13}C_{org}$ were measured on aliquots of rinsed and dried residues of acid digestion by combustion to CO_2 on an ECS 4010 Elemental Analyzer (Costech Analytical Technologies Inc., Valencia, California, USA) and measured on a Thermo Fischer Delta V Plus Isotope Ratio Mass Spectrometer (Thermo Fisher Scientific) at Washington University. Values are reported in per mil (‰) relative to the Vienna Pee Dee belemnite (VPDB) standard. TOC was determined by comparing the area of the evolved CO_2 peak to standards run at varied masses and corrected for the carbonate content of the sample. A total of 151 samples were analysed for $\delta^{13}C_{org}$. Average standard deviations (1σ) for $\delta^{13}C_{org}$ standards USGS 24 (graphite), IAEA CH-6 (sucrose) and IAEA CH-3 (cellulose) were 0·11‰, 0·14‰ and 0·13‰, respectively.

Elemental abundance

Samples were prepared for inductively coupled plasma optical emission spectrometry (ICP-OES) on an Optima 7300DV ICP-OES (Perkin-Elmer Inc., Waltham, Massachusetts, USA) at Washington University. Approximately 1·0 mg of carbonate powder was dissolved in 10% (Optima grade) acetic acid or with 5% HNO_3 (Optima grade) in 15 ml Falcon centrifuge tubes. Samples were placed on a shaker table and left to dissolve overnight. Samples were filtered through a 0·2 μm nylon filter prior to analysis. Standards were run at 1, 10, 20, 50, 100 and 500 ppb concentrations for Mn and Sr, while Ca and Mg were run using 1, 10, 50 and 100 ppm standards. Costech multi-element standards were used in combination with single element standards with no first-order spectral interferences. Standards for Ca, Mg, Mn, and Sr had an average reproducibility (1σ) of <1% across concentrations. The spectral lines used were Ca = 317·933 nm, Mg = 279·077 nm, Mn = 257·61 nm and Sr = 407·771 nm.

PETROGRAPHIC, SEDIMENTOLOGICAL RESULTS & INTERPRETATIONS

Plattin Limestone

Observations

The upper Plattin Limestone consists of the Macy and Castlewood Members. The Macy Member is composed of thin-bedded to medium-bedded, heavily burrowed mudstones and wackestones with occasional grainstone lenses (Figs 3A, 4A and 4B). When weathered, differential cementation of burrows and surrounding sediment imparts a 'Swiss cheese-like' appearance to the rock. The overlying Castlewood Limestone is heavily bioturbated, thick to massively bedded with occasional stylolites. Burrows in the Plattin are large (*ca* 2 cm diameter) and pastel-yellow (Fig. 4A) or brown-grey (Figs 3A and 4A). Burrows are filled with euhedral dolomite crystals 20 to 100 μm in diameter set in a fine-grained calcite matrix (Fig. 5A). Dolomite abundance is positively correlated to bioturbation intensity, which decreases stratigraphically up within the Plattin Group. Thin section analysis shows dolomite abundance decreasing to <1% (by area) a few millimetres away from burrows. In general, bioclastic lenses and matrix materials were predominantly calcite. Plattin strata occasionally contain identifiable bryozoa, echinoderm fragments and trilobites set in a calcite micrite matrix. Fossil texture preservation was poorer relative to the Decorah Formation and average whole fossil size was smaller in the Plattin Limestone relative to other units in this study.

Interpretation

The Plattin Limestone is interpreted to represent a sub-tidal environment with stable sea-level conditions that terminated with the upward shoaling Castlewood Member. The small grain size and high burrow abundance is interpreted to represent deposition in oxygenated, intermittently calm conditions, while the absence of

evaporites and obvious subaerial exposure features are in agreement with a consistently submerged subtidal environment.

Glencoe Shale

Observations

The Glencoe Shale is composed of dark green to grey, thinly bedded, fissile shales and deep blue to purple calcarenites and calcirudites (Figs 4B and 5B) that sometimes pinch out over decimetres to metres. Occasional bioclastic beds were present (Fig. 5C). Sedimentological structures (for example, cross-bedding and grading) and burrows were uncommon. Scouring created cm-scale relief in some beds. Dolomite is absent or in trace amounts throughout most of the matrix, but is found in yellow, red and green diagenetic textures associated with bedding planes and burrow fill. Thin section analyses showed clasts to be supported in a granular cement fabric with higher total cement content found in finer-grained grainstones. The Glencoe Shale was nearly twice as thick at Highway MM compared to New London with a larger amount of shale found at Highway MM. The boundary between the Glencoe Shale and overlying Kings Lake Limestone is more abrupt at Highway MM and marked by a significant reentrant, while the lithological transition is more gradational at New London.

Interpretation

The Glencoe Shale formed in a shallow sub-tidal environment (Thompson, 1991). The presence of shales and calcareous tempestites suggests calm-water conditions punctuated by high-energy storm events that brought in allochthonous bioclasts.

Kings Lake Limestone

Observations

The Kings Lake Limestone differs lithologically between sections. The entirety of the Kings Lake at New London and the interval from the base of the Kings Lake to just above HMKL-1 at Highway MM is made of blue-grey wackestones and grainstones (Figs 3B, 4C, 4D and 4E) with abundant thin shale partings. Above HMKL-1 the Kings Lake Limestone is more mud rich (Fig. 4). Fossils are abundant in hand sample and thin section throughout the entire Kings Lake and include trilobites, brachiopods, ostrocods and bryozoa (Figs 4D and 5D), while rare crinoid stalks were found in shale partings. At New London, the Kings Lake contact with the overlying Guttenberg Limestone occurs just above a bentonite horizon (NLKL-1). The contact between the Kings Lake and Kimmswick Limestones at Highway MM has relief up to 7 cm with possible evidence for karstification in the uppermost 30 cm of the Kings Lake. A potential hardground was identified 15 cm below the Kimmswick contact (Fig. 4G). In both locations, the Kings Lake contains little dolomite (<3%), except in the 'wispy brushstroke' textures, which are only found at Highway MM (Fig. 4F) and which vary in dolomite concentration up to *ca* 40%.

Interpretation

The Kings Lake Limestone was deposited during transgression in a sub-tidal, shallow sea, likely distal to a siliciclastic sediment source. At Highway MM, the Kings Lake represents a wider range of depositional environments than at New London, as evidenced by the lithological differences above and below HMKL-1. Hereafter, the zones above and below HMKL-1 are referred to as the Lower and Upper Kings Lake, respectively. The transition to higher mud content and increased fossil preservation in the Upper Kings Lake (Highway MM) is interpreted to represent deposition in the deepest and most distal water facies at this location, similar to conditions ascribed to the Guttenberg Limestone at New London. The Lower Kings Lake at Highway MM is lithologically correlative with all of the Kings Lake at New London, while the Upper Kings Lake is lithologically equivalent with the Guttenberg Limestone at New London (see below).

Guttenberg Limestone

Observations

The Guttenberg Limestone is only found at New London and is lithologically similar to the Upper Kings Lake Limestone at Highway MM. This is seen in the mudstones and wackestone–packstone tempestites of the Upper Kings Lake (Highway MM) and Guttenberg (New London) (Fig. 3C, D and E), except that Guttenberg Limestone mud and shale fractions are brown (rather than blue), which is correlated with higher TOC content. Macrofossils and microfossils are abundant (Fig. 3C and D), while spar and dolomite abundances are low. Burrowing textures are common, but textures are less obvious in hand sample relative to other units in this study. Low-angle cross-laminations were observed in

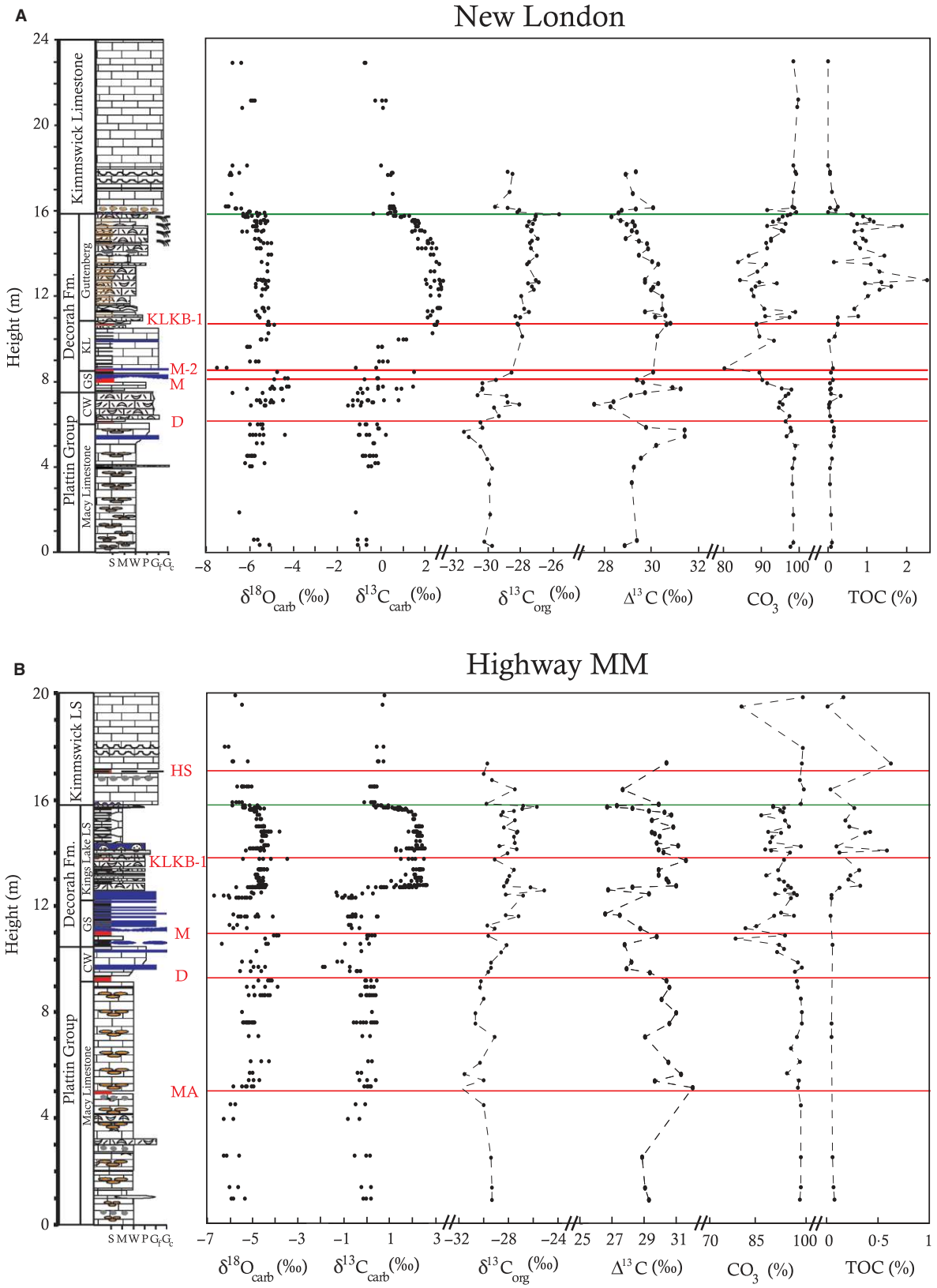

Fig. 6. Isotopic and geochemical data for New London (top) and Highway MM (bottom). $\delta^{13}C_{carb}$ and $\delta^{18}O_{carb}$ are microdrilled samples. All other values are bed-averaged (Tables S1 and S2). Isotopic data are reported in ‰ relative to VPDB.

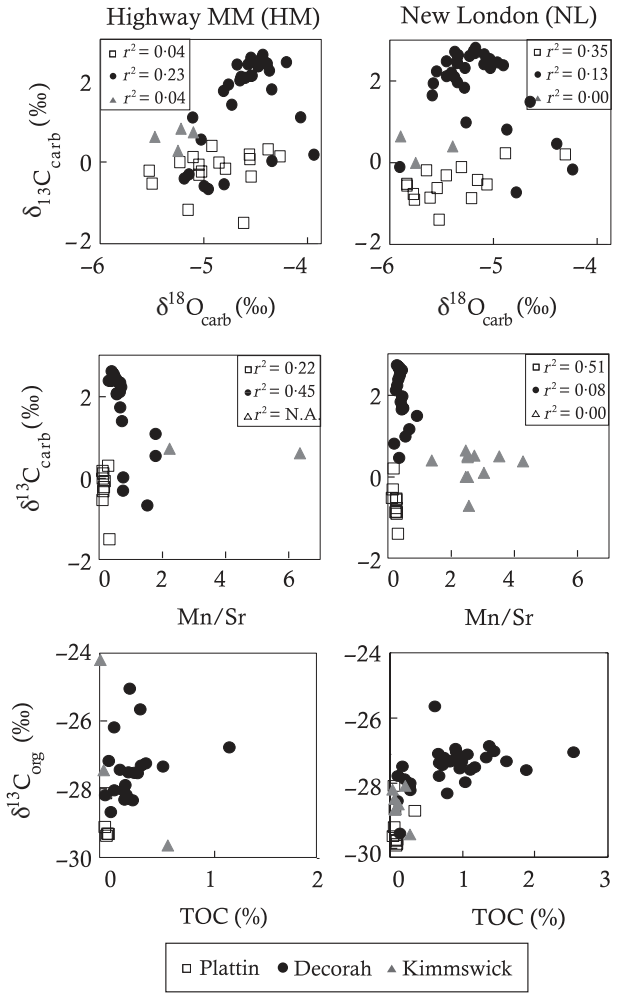

Fig. 7. Geochemical cross-plot results for New London (left) and Highway MM (right). Values are isotope-texture screened and $\delta^{18}O_{carb}$ filtered (see *Methods*). r^2 corresponds to linear least-squares fit; see Tables S1 and S2 for values. $\delta^{13}C_{carb}$, $\delta^{13}C_{org}$ and $\delta^{18}O_{carb}$ values are reported in ‰ relative to VPDB.

the upper 1 to 2 m with lighter laminations corresponding to coarser grain sizes, decreased organic content and increased cement abundance (Fig. 3E). The Guttenberg Limestone is unconformably overlain by the Kimmswick Limestone with a few centimetres of erosional relief present at the contact.

Interpretation

Similar to the Kings Lake Limestone, the Guttenberg Limestone formed in a shallow epeiric sea distal to siliclastic sediment sources. Lithological similarities between the Guttenberg at New London and the Upper Kings Lake at Highway MM argue for similar depositional and environmental characteristics. This also suggests that the Upper Kings Lake and Guttenberg may be partially time-equivalent. There is no evidence to support erosion of the Guttenberg Limestone south of St. Louis as previously reported (Thompson, 1991; Kolata *et al.*, 1998).

Kimmswick Limestone

Observations

The Kimmswick Limestone is a heavily burrowed, fine to coarse-grained limestone and appears somewhat saccharine in outcrop. The dominant mineral is calcite with up to 1 to 3% disseminated dolomite in a granular mosaic cement fabric (*sensu* Flügel, 2009). Grains are dominantly bioclastic. Burrows contain variable dolomite concentrations with darker, better-defined burrows bearing the highest dolomite concentrations (up to *ca* 40% dolomite) (Fig. 4H). The lowermost 20 cm of the Kimmswick contains large (up to 10 cm) rip-up clasts from the underlying Guttenberg (at New London) (Fig. 3F) and Upper Kings Lake (at Highway MM) strata.

Porosity is highest in the upper portions of the Kimmswick where pores are lined by a chalky yellow dolomitic material. While Kimmswick burrow structures are similar to those of the Plattin Limestone, the burrow walls are not as well defined and overall mud content is much lower (Figs 3G and 4H). Cross-bedding was not observed in this study, but has been reported stratigraphically farther up the Kimmswick from a section near Barnhart, Missouri (Thompson, 1991).

Interpretation

The Kimmswick Limestone marked a return to a higher energy environment impacted by wave-tide action, consistent with the presence of fragmented bioclasts and mud-poor composition. The nature of the contact (including rip-up clasts) with the underlying Guttenberg Limestone (New London) and Kings Lake Limestone (Highway MM) is also consistent with a transition to a higher energy environment with the onset of Kimmswick deposition. The stratigraphically thick, monotonous grainstones of the Kimmswick Limestone suggest consistent environmental conditions during deposition.

GEOCHEMICAL RESULTS

Stratigraphic trends

Overall, $\delta^{13}C_{carb}$ and $\delta^{18}O_{carb}$ values range from −2 to 3‰ and −8 to −4‰, respectively, with

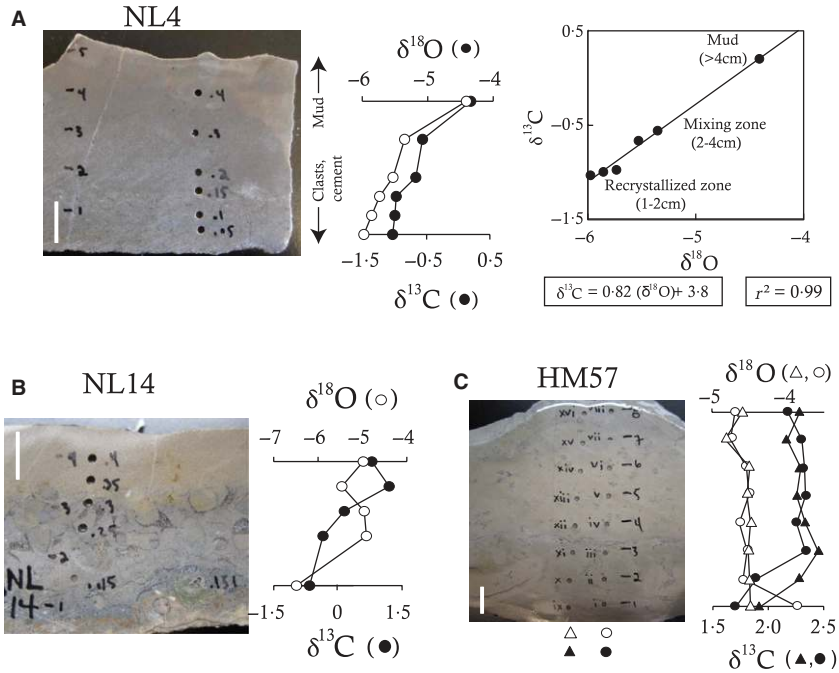

Fig. 8. Vertical and lateral trends in $\delta^{13}C_{carb}$ (black symbols) and $\delta^{18}O_{carb}$ (white symbols) in hand samples. Multiple transects are split by symbol type (left = triangles, right = circles). All values are reported in ‰ relative to VPDB. Scale bar (white) is 1 cm. (A) Calcarenite grading upwards to mudstone NL4. Linear regression of NL4 showing correlation in $\delta^{13}C_{carb}$ and $\delta^{18}O_{carb}$. Strong correlation results from linear mixing of a coarser, cement-rich component in base of rock with an isotopically heavier mud component near the top. Sample contains <1% dolomite. (B) Wackestone-Packstone NL14. Vertical enrichment primarily results from increasing fractions of isotopically heavy mud, but contains more than two isotopically distinct components. (C) Mudstone HM57. Lower $\delta^{13}C_{carb}$ and higher $\delta^{18}O_{carb}$ at bottom result from mixing with 'wispy brushstroke' texture, which contains abundant dolomite and affects the bulk isotope signals in the lower 2 cm.

similar profiles in both sections (Fig. 6; Table S1 (New London); Table S2 (Highway MM). The Guttenberg excursion dominates the $\delta^{13}C_{carb}$ profile, rising from a baseline of $\delta^{13}C_{carb}$ near 0‰ in the base of the Kings Lake Limestone to a peak of 3‰ in the middle Kings Lake Limestone (Highway MM) and Guttenberg Limestone (New London), before returning to 0‰ in the Kimmswick Limestone (Fig 6). In addition, there is a small (1 to 2‰) negative excursion in $\delta^{13}C_{carb}$ found across the Deicke K-bentonite. $\delta^{18}O_{carb}$ averages –5·5‰ and –5‰ for New London and Highway MM, respectively, with lower values in the Glencoe Shale (Highway MM only), Kings Lake Limestone (New London only) and Kimmswick Limestone. A rise in $\delta^{18}O_{carb}$ accompanies the rising limb of the $\delta^{13}C_{carb}$ Guttenberg excursion at both localities, while a less-pronounced fall in $\delta^{18}O_{carb}$ is paired with the falling limb of the Guttenberg excursion only at Highway MM.

Superimposed on these first-order trends is permil-level scatter associated with different textures and mineralogy. Spar, single large clasts and cement-rich and microclast-rich zones typically had lower $\delta^{13}C_{carb}$ and $\delta^{18}O_{carb}$, while dolomite-rich regions had variable $\delta^{13}C_{carb}$ and $\delta^{18}O_{carb}$, depending upon formation and texture. For example, yellow dolomitic burrow fill in the Plattin Limestone had $\delta^{13}C_{carb}$ values similar to the calcitic matrix and elevated in $\delta^{18}O_{carb}$ by 0·2 to 0·9‰, while the smoky grey dolomite-rich zone in the same formation had $\delta^{13}C_{carb}$ values and $\delta^{18}O_{carb}$ up to 4‰ and 0·4‰ higher, respectively. Geochemical analysis ([Ca]/[Mg] ratios and [Sr] values) and thin section observations support the link between observed isotopic variability and dolomitization and/or secondary cementation. Samples with significant dolomite (>5%) were omitted from stratigraphic correlation.

Isotopic variability can occur in data across multiple spatial scales from the individual hand sample to the formation level. Secondary carbonates of meteoric origin often contain lower $\delta^{13}C_{carb}$ and $\delta^{18}O_{carb}$ values than primary material (e.g. Allan & Matthews, 1982; Veizer *et al.*, 1997, 1999; Brand, 2004) and high-temperature calcite has a lower $\delta^{18}O_{carb}$ signature owing to the strongly temperature-dependent fractionation of oxygen isotopes during calcite precipitation

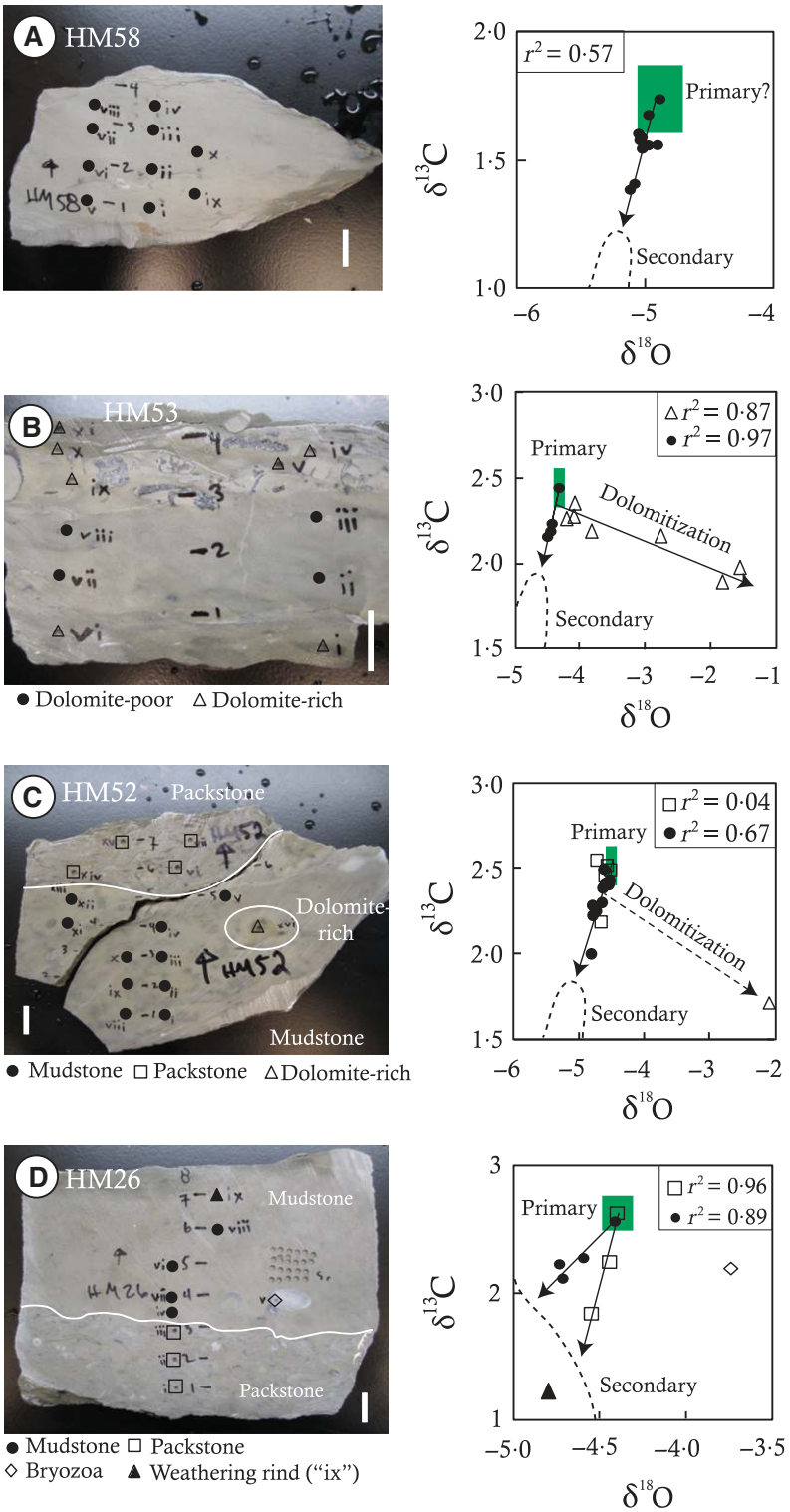

Fig. 9. Plots of $\delta^{13}C_{carb}$ vs. $\delta^{18}O_{carb}$ for single hand samples. All values are reported in ‰ relative to VPDB. Scale bar (white) is 1 cm. Filled green rectangles show 2σ error ($\delta^{13}C_{carb}$ = 0·18‰, $\delta^{18}O_{carb}$ = 0·26‰) and represent inferred 'primary' values. 'Dolomitization' refers to the trend for increasing amounts of dolomite in microdrilled samples; 'secondary' refers exclusively to non-primary calcite. (A) Mudstone HM58 showing typical two-component mixing line. (B) Wackestone HM53 showing three components. (C) Mudstone-packstone HM52 showing similar trends to HM53. (D) Mudstone-Packstone HM26 showing different mixing line slopes. Convergence upon a single value is consistent with both lithologies in the sample having common primary $\delta^{13}C_{carb}$ and $\delta^{18}O_{carb}$ values with differing diagenetic histories associated with the different Dunham classification.

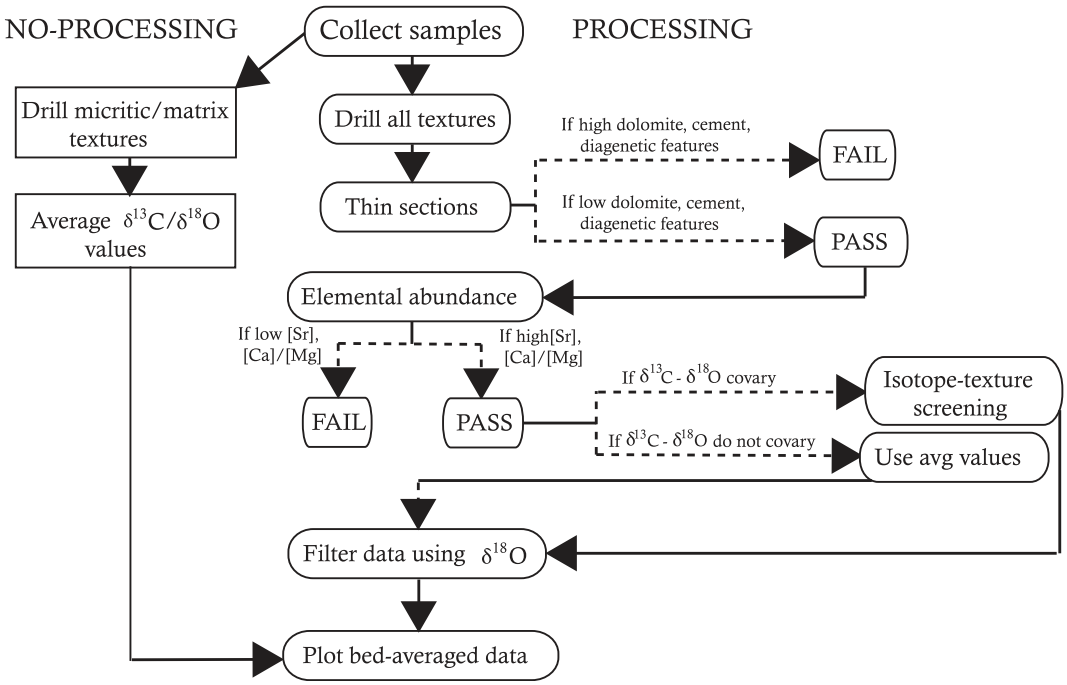

Fig. 10. Decision tree for isotope-texture screening and $\delta^{18}O_{carb}$ filtering.

(Epstein & Mayeda, 1953). To test for the influence of secondary phases of meteoric origin, $\delta^{13}C_{carb}$ versus $\delta^{18}O_{carb}$ cross-plots were constructed (Fig. 7). Data were divided into the three main stratigraphic units: the Plattin, Decorah and Kimmswick. No consistent formation-scale covariance patterns were observed between sections.

The $\delta^{13}C_{org}$ values ranged from −33 to −24‰ (Fig. 6); $\delta^{13}C_{org}$ is most negative beneath the Deicke K-bentonite and peaks in the Guttenberg (New London) (Fig. 6A) and Kings Lake Formations (Highway MM) (Fig. 6B). From the initial baseline values in the Plattin Limestone, $\delta^{13}C_{org}$ increases twice, once each across the Deicke and Millbrig K-bentonites, above which it steadily rises up to the contact with the Kimmswick Limestone. $\delta^{13}C_{org}$ rapidly returns to pre-excursion values (−30‰) in the basal Kimmswick. The isotopic offset between carbonate carbon and organic carbon, $\Delta^{13}C$ (=$\delta^{13}C_{carb} - \delta^{13}C_{org}$), shows no systematic relation between sections except in the interval from the HMKL-1/NLKL-1 bentonite to the Kimmswick contact, where $\Delta^{13}C$ steadily decreases from 30 to 29‰ (Fig. 6).

Total organic carbon is less than 0·2% in most of the Plattin Limestone, Glencoe Shale and Kimmswick Limestone. Highest TOC values are found in the Decorah Formation (0·6% at Highway MM, 2·5% at New London). In contrast, carbonate content was highest in the Plattin Limestone and Kimmswick Limestone and lowest in the Decorah Formation. Two intervals of decreased carbonate content are observed: one near the Millbrig K-bentonite and the other, a few metres above the HMKL-1/NLKL-1 bentonite (Fig. 6).

Strontium concentrations ([Sr]) were consistent and averaged *ca* 300 ppm in the Plattin Limestone. [Sr] also averaged *ca* 300 ppm in the Glencoe Shale, increased to around 1,000 ppm in the Lower Kings Lake Limestone (Highway MM only) and Guttenberg Limestone (New London only), and consistently averaged *ca* 200 ppm in the Kimmswick Limestone (Tables S1 and S2). Formational averages were similar between sections. Microdrilling results show dolomite-rich and recrystallized zones had decreased [Sr].

In summary, geochemical characteristics show little variation throughout the Plattin (with the exception of the Castlewood Limestone) and Kimmswick Limestones (Fig. 6). These units are characterized by low TOC, [Sr], $\delta^{13}C_{carb}$, $\delta^{13}C_{org}$, $\delta^{18}O_{carb}$ and high carbonate purity. This homogeneous geochemical profile is paralleled by the observed lithological homogeneity in these units. Geochemical patterns show clear signals of increasing $\delta^{13}C_{carb}$, TOC, [Sr] and decreasing % carb in the Decorah Formation. Within the Decorah the Upper Kings Lake Limestone at Highway MM has geochemical trends similar to those seen

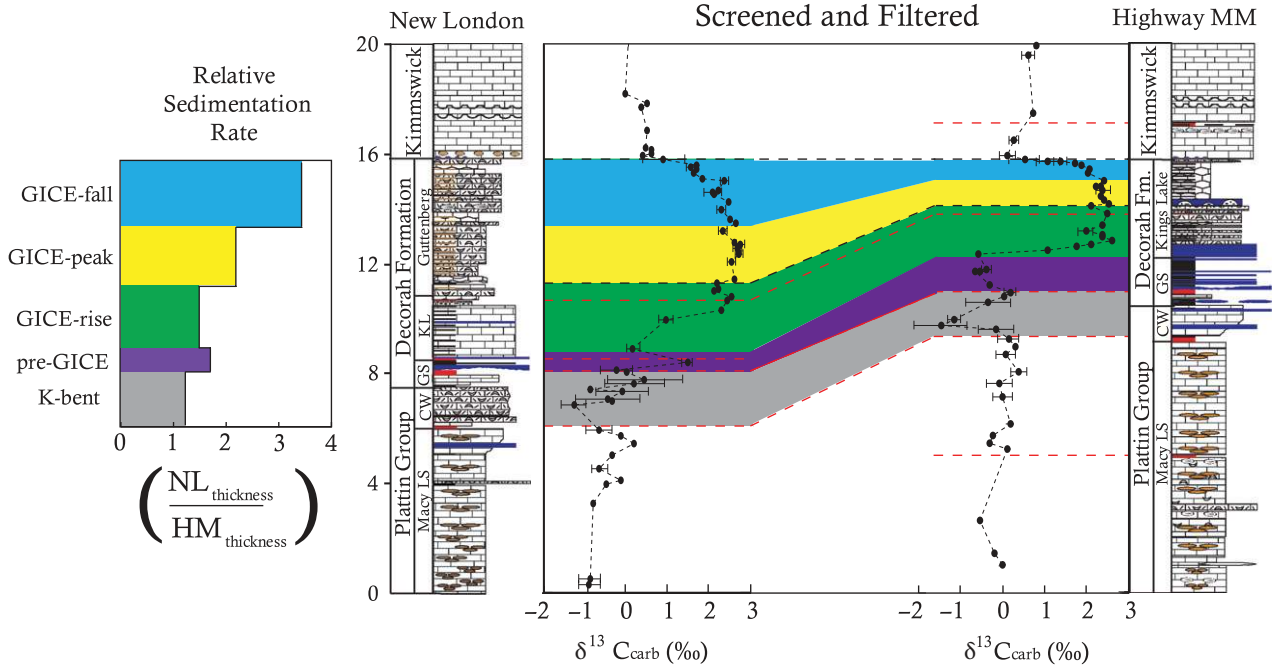

Fig. 11. $\delta^{13}C_{carb}$ correlations with screened and filtered data across the Guttenberg isotopic carbon excursion (GICE). Height is in metres. Colours correspond to chonostratigraphic intervals. 'K-bent' chronozone is bounded by K-bentonites and independent of $\delta^{13}C_{carb}$. The remaining intervals are defined by $\delta^{13}C_{carb}$ chemostratigraphy. Bar graph shows relative sedimentation rate (RSR) of New London relative to Highway MM. Error bars represent standard deviation (1σ) of bed-averaged values.

in the Guttenberg Limestone of New London (Fig. 6), but with lower TOC. The geochemical similarities between the Upper Kings Lake Limestone (Highway MM) and Guttenberg Limestone (New London) are consistent with the lithological similarities for the same strata.

Intra-bed $\delta^{13}C_{carb}$ and $\delta^{18}O_{carb}$ variability

Centimetre-scale drilling transects were completed to assess small-scale $\delta^{13}C_{carb}$ and $\delta^{18}O_{carb}$ variability within individual samples to better constrain primary signatures used for correlation and carbon cycle reconstruction. These results revealed significant isotopic heterogeneity within single beds (Fig. 8) and many samples showed vertical increases in $\delta^{13}C_{carb}$ and $\delta^{18}O_{carb}$ over just a few centimetres (Fig. 8A and B), while isotopic scatter in other samples was restricted to bedding planes (Fig. 8C). Excluding heavily dolomitized zones and other obviously altered textures, the magnitude of change within individual beds in $\delta^{13}C_{carb}$ was up to 2·0‰, while the change in $\delta^{18}O_{carb}$ was up to 3·0‰. This isotopic variability was sometimes related to lithological transitions. For example, in Plattin sample NL4 (Fig. 8A), a fine-grained calcarenite that grades upward to a mudstone, $\delta^{13}C_{carb}$ was 1‰ higher and $\delta^{18}O_{carb}$ was 1·6‰ higher in the mudstone portion. These data fell along a mixing line (r^2 = 0·99, n = 6) and correlate with cement content and grain size.

Drilling transects across differing textures (Fig. 9) allowed the identification of component mixing where dolomite, cement and clasts influenced bulk isotope signatures. Coupled petrographic and isotopic analyses showed the highest $\delta^{13}C_{carb}$ and $\delta^{18}O_{carb}$ samples to be muds and dolomite-rich zones while cements and recrystallized materials had the lightest $\delta^{13}C_{carb}$ and $\delta^{18}O_{carb}$ (for example, Fig. 8A). A linear $\delta^{13}C_{carb}$ to $\delta^{18}O_{carb}$ trend is then an isotope mixing line where points on the line represent gradational changes in the relative proportions of two components. This logic was the basis for constructing an 'isotope-texture screen' to select the 'least-altered' $\delta^{13}C_{carb}$ and $\delta^{18}O_{carb}$ values from populations within single samples.

In some cases, plots showed changes in $\delta^{13}C_{carb}$ while $\delta^{18}O_{carb}$ was invariant. For example, brown Guttenberg mudstones-packstones had higher $\delta^{13}C_{carb}$ in darker brown micrite and lower $\delta^{13}C_{carb}$ in light brown micrite while $\delta^{18}O_{carb}$ was constant. Petrographic analyses revealed a larger average crystal size, a likely diagenetic feature, in lighter shades of micrite that corresponded with

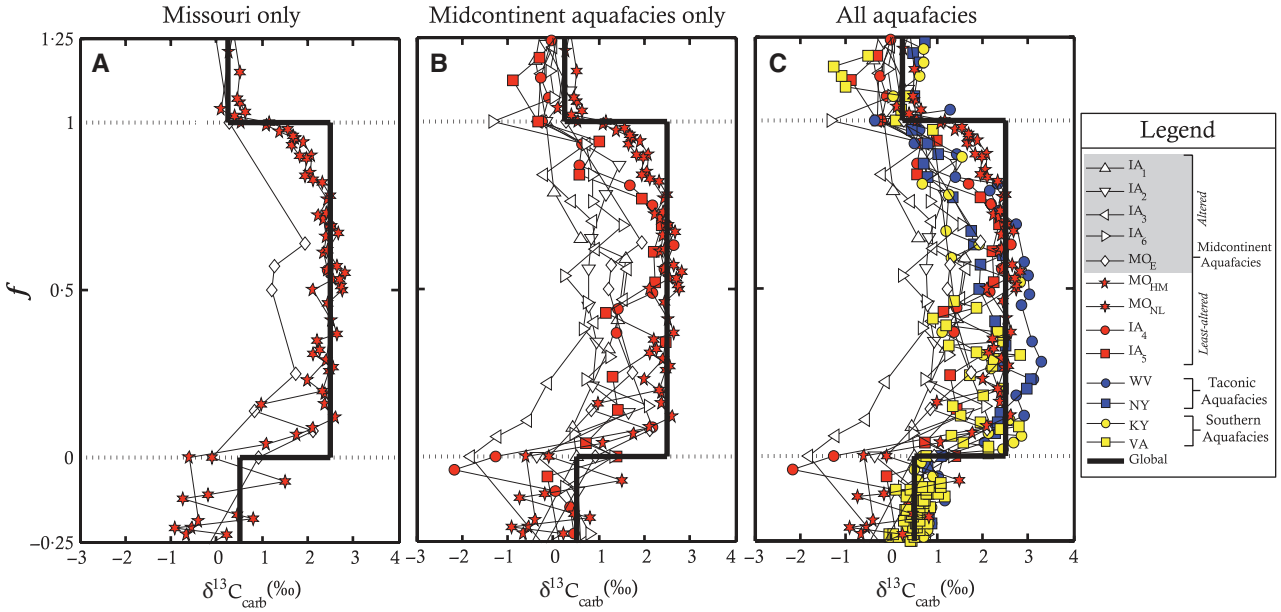

Fig. 12. Plot of normalized Guttenberg $\delta^{13}C_{carb}$ excursions in Laurentian sections where the duration of the excursion is normalized from 0 to 1, with 0 defined as the beginning of the excursion and 1 as the end. Generalized global $\delta^{13}C_{carb}$ values (heavy solid line) for the pre-Guttenberg, peak-Guttenberg and post-Guttenberg excursion taken from Bergström *et al.* (2009b). Instrumental error (1 standard deviation) is less than symbol size. (A) Normalized excursions for Missouri (MO) sections. Eureka (MO_E, black diamonds) from Ludvigson *et al.* (2000), Highway MM (MO_{HM}, red pentagrams) and New London (MO_{NL}, red hexagrams) from this report. (B) Normalized excursions 'Midcontinent aquafacies'. Iowa (IA) subscripts refer to sample localities of Ludvigson *et al.* (2004). Note the general agreement in pre- Guttenberg, peak- Guttenberg, and post-Guttenberg excursion values and lower degrees of scatter in least-altered sections compared to altered sections. (C) Normalized excursions for all aquafacies with aquafacies designations taken from Young *et al.* (2005). Data for Virginia (VA), West Virginia (WV) and Kentucky (KY) from Young *et al.* (2005). New York (NY) data is unpublished.

lower $\delta^{13}C_{carb}$, therefore the higher $\delta^{13}C_{carb}$ values from darker zones were taken as more representative of primary $\delta^{13}C_{carb}$. When no petrographic or geochemical evidence could indicate which textures/phases were most primary, an average of all values was taken.

$\delta^{18}O_{carb}$ filter

While the 'isotope-texture screen' is useful in identifying the 'least-altered' values within a single sample, it does not necessarily help in deciding whether those values are themselves well-suited for chemostratigraphic correlation. To address this problem, samples can be filtered using their $\delta^{18}O_{carb}$ value. $\delta^{18}O_{carb}$ filtering is done by excluding samples with $\delta^{18}O_{carb}$ values below a certain threshold where the threshold is defined as some value below the mean $\delta^{18}O_{carb}$ value for samples that passed the 'isotope-texture' screen for a given formation. The $\delta^{18}O_{carb}$ cutoff value was arbitrarily picked as one standard deviation (1σ) lighter than the formational average. The $\delta^{18}O_{carb}$ cutoff values for each formation can be found in Table S3.

Hereafter, correlations and environmental reconstructions use only $\delta^{13}C_{carb}$ data that passed isotope-texture screening *and* $\delta^{18}O_{carb}$ filtering. A decision tree (Fig. 10) shows the process used to construct these 'least-altered' $\delta^{13}C_{carb}$ values. The full list of samples along with information as to whether they pass or fail the isotope-texture screening and $\delta^{18}O_{carb}$ filter can be found in Tables S1 and S2.

DISCUSSION

Intra-sample geochemical variability

Variations in bulk $\delta^{13}C_{carb}$ values within and between individual samples can result from analysing mixtures of two or more isotopically distinct components (i.e. mud, cement and clasts). This was elegantly demonstrated by Swart (2008) who showed that Cenozoic periplatform and ramp $\delta^{13}C_{carb}$ values were decoupled from open ocean signal due to mixing of isotopically distinct aragonite from the shallow platform with pelagic calcite materials. As

shown in Figs 8 and 9, varying mixtures of mud, clasts, cements and dolomite explain much of the isotopic variability within individual hand samples. The largest range in $\delta^{13}C_{carb}$ values within an individual sample was greater than 2·0‰ (equal to *ca* 80% of the magnitude of the Guttenberg excursion), highlighting the importance of both sample screening and high-resolution data for stratigraphic correlation and palaeoenvironmental or palaeoceanographic reconstructions. From these results, it is apparent that $\delta^{13}C_{carb}$ and $\delta^{18}O_{carb}$ scatter within a single sample is often unrelated to a primary marine (i.e. water column) environmental signal and, instead, reflects the mixing of diagenetic components and primary materials. This framework provides an objective criterion for the selection of the 'least-altered' $\delta^{13}C_{carb}$ values.

Because secondary carbonates often contain lower $\delta^{13}C_{carb}$ and $\delta^{18}O_{carb}$, the heaviest $\delta^{13}C_{carb}$ values are usually considered more primary (Fig. 9A). For this work, accepting only the heaviest $\delta^{13}C_{carb}$ would lead to incorporation of substantial diagenetic artifacts because dolomite-rich samples occasionally had $\delta^{13}C_{carb}$ signatures and frequently had $\delta^{18}O_{carb}$ signatures heavier than the reconstructed 'least-altered' values. When dolomite was present, plots with two linear mixing lines provided an objective argument for choosing most-primary $\delta^{13}C_{carb}$ and $\delta^{18}O_{carb}$ values (for example, Fig. 9B and C).

Not all of the samples characterized fell along a linear mixing line. This may be the result of multi-component mixing (for example, Fig. 9B, C and D), natural environmental variation, or cryptic diagenetic alteration; samples that showed poor covariation across $\delta^{13}C_{carb}$ and $\delta^{18}O_{carb}$ over a range in excess of analytical precision are believed to result from one of these causes. For example, Fig. 9D shows two intersecting mixing lines for the mudstone and packstone portions of sample HM26. The intersection of these two lines is interpreted to represent primary $\delta^{13}C_{carb}$ and $\delta^{18}O_{carb}$ signatures for all components, while the different downward trajectories represent the inclusion of different secondary cements possibly relating to different diagenetic histories. Such scatter prevented development of a well-constrained dolomite-rich $\delta^{13}C_{carb}$ and $\delta^{18}O_{carb}$ signature and is thought to result either from multiple generations of dolomite and/or calcite cement that precipitated under different conditions or from variable amounts of calcite/dolomite within the dolomitized zone. In such cases, 'least-altered' samples were selected based on qualitative trends in the $\delta^{13}C_{carb}$–$\delta^{18}O_{carb}$ sample population.

Centimetre-scale isotope transects revealed that *the majority* of samples had isotopic offsets arising from variable amounts of secondary material. Only 2 of 11 samples (18%) were identified as 'least altered' in Fig. 9A, demonstrating that *most* samples carried a significant secondary signal (i.e. offset from 'primary' by more than twice instrumental precision). The impact of secondary alteration on $\delta^{13}C$ and $\delta^{18}O$ may be further tested on the micron-scale using secondary ion mass spectrometry (SIMS) or similar instruments to allow for grain-specific isotope analysis. In sum, confident identification of 'least-altered' components requires a combination of petrographic, elemental abundance and isotopic analyses, particularly when the magnitude of intrabed $\delta^{13}C_{carb}$ variability is similar to that of the stratigraphic signal being investigated.

$\delta^{18}O_{carb}$ filter

A $\delta^{18}O_{carb}$ filter was applied to all samples that passed the above isotope-texture screening. This filter was designed to exclude samples subjected to pervasive resetting of $\delta^{18}O_{carb}$ such as would occur during meteoric diagenesis. The $\delta^{18}O_{carb}$ isotope filter provides an objective criterion for formation-scale sample discrimination in isotopically heterogeneous rocks, provided careful petrographic and chemical characterization has been done. Because $\delta^{18}O_{carb}$ is easier to reset than $\delta^{13}C_{carb}$ during diagenesis (Lohmann, 1988), a $\delta^{18}O_{carb}$ filter provides a conservative method for isolating 'least-altered' $\delta^{13}C_{carb}$ data. Without $\delta^{18}O_{carb}$ filtering, some $\delta^{13}C_{carb}$ data sets may be artificially noisy and the resulting chemostratigraphic correlations and environmental reconstructions may be misleading or inaccurate.

While careful screening and filtering can aid in arriving at a 'least-altered' $\delta^{13}C_{carb}$ profile a small number of samples that displayed clear textural evidence of post-depositional alteration would have passed both the isotope-texture screening and the $\delta^{18}O_{carb}$ filter. This demonstrates that the isotope-texture and $\delta^{18}O_{carb}$ filters remain imperfect screens for identifying alteration and that petrographic and trace element abundance data should be considered. Some beds yielded $\delta^{13}C_{carb}$ values different than those from beds above and below representing a break in a stratigraphically consistent $\delta^{13}C_{carb}$ pattern. If these aberrant $\delta^{13}C_{carb}$ values were primary, they would represent a complex and rapidly changing global car-

bon cycle (Kump & Arthur, 1999), but it is mechanistically simpler to invoke alteration by diagenetic fluids. While no samples in this work were discarded based on stratigraphic continuity of $\delta^{13}C_{carb}$ alone this may be sufficient evidence to omit samples in other studies. If done, care should be taken to avoid a model-driven interpretation of data that excludes real negative excursions in $\delta^{13}C_{carb}$.

$\delta^{13}C$ chemostratigraphic correlations and relative sedimentation rates

Figure 11 shows the proposed chemostratigraphic relations between Localities Highway MM and New London using $\delta^{13}C_{carb}$ data that passed both the isotope-texture screen and $\delta^{18}O_{carb}$ filter. The Guttenberg excursion is a conspicuous feature of the $\delta^{13}C_{carb}$ profile at both sections, where it is preserved as a *ca* 2·5‰ positive excursion, a magnitude similar to those previously reported from other Laurentian sections (Bergström *et al.*, 2010a). The continuity of the $\delta^{13}C_{carb}$ signal throughout the Guttenberg excursion at Highway MM suggests that the Guttenberg Limestone was never deposited at Highway MM and that any erosion was less substantial than previously thought (Kolata *et al.*, 1986, 1987; Thompson, 1991) as the Guttenberg Limestone is the member that contains the Guttenberg excursion in northern Missouri. A comparison of $\delta^{13}C_{carb}$ profiles shows that the difference in thickness of the Kings Lake Limestone between New London and Highway MM and the absence of the Guttenberg Limestone at Highway MM can be best explained if the Upper Kings Lake Limestone (Highway MM) is a synchronous southern facies equivalent of the Guttenberg Limestone (New London). Figure 12A shows the Guttenberg excursion curve for Missouri sections normalized for excursion duration. The similarity in morphologies between Highway MM and New London during the falling stage of the Guttenberg excursion shows that sedimentation at Highway MM was as continuous as that at New London, but slower. This provides further evidence against erosion of the Guttenberg time-equivalent strata at Highway MM as erosion would produce a different normalized excursion morphology. These data are in strong agreement with lithological and geochemical observations.

Comparison of relative sedimentation rate (RSR) between localities can be used to understand spatial differences in deposition rates. The RSR is a unitless ratio of lithological thickness of a given $\delta^{13}C_{carb}$ interval from one section to another (here the ratio of stratigraphic thickness in New London strata relative to that in Highway MM strata). In the present case, the intervals are defined by a combination of K-bentonites and features in the $\delta^{13}C_{carb}$ profiles (Fig. 11). In this manner, the isotopes reveal the partitioning of time between units and show the geographic relation in relative sedimentation rates. The RSR is near unity during the 'K-bent' chronozone and through the onset of the Guttenberg excursion, arguing for similar sedimentation rates at Highway MM and New London. The RSR increases above the HMKL-1/NLKL-1 bentonite near peak Guttenberg excursion $\delta^{13}C$ values, as net sedimentation rates at New London outpaced those at Highway MM. A possible hardground 15 cm below the Kimmswick contact at Highway MM suggests that sedimentation was very condensed at this locality but, as Fig. 12A shows, not so condensed as to significantly change the normalized excursion morphology at Highway MM. Lack of evidence for subaerial exposure is consistent with a continuously submerged environment at Highway MM and that the high RSR resulted, at least in part, from declining sediment production rates and/or a decrease in the creation of new accommodation space at this location. The shift in RSR is roughly coincident with the start of the Taconic Orogeny (Rodgers, 1971), and the differential subsidence may be the result of a far-field tectonic forcing on the inner craton (see discussion in Holland & Patzkowsky, 1998) or changing regional tectonics related to the Ozark Dome. Future development of robust correlations in the overlying Kimmswick Limestone could test whether these sedimentation patterns continue in younger strata.

$\delta^{13}C_{org}$

Sedimentary organic carbon is filtered through a complex network of biological processing during carbon fixation, heterotrophic reworking and microbial respiration. As such, the $\delta^{13}C_{org}$ signal reflects not only variations in $\delta^{13}C$ from the parent dissolved inorganic carbon (DIC) source, but also changing ecological and environmental (for example, facies-dependent) factors. Therefore, fractionation can be influenced strongly by local signals and resulting interpretations of $\delta^{13}C_{org}$ data are less straightforward than $\delta^{13}C_{carb}$ (Hayes

et al., 1999). The Guttenberg excursion is weakly expressed in $\delta^{13}C_{org}$, where the signal is either superimposed over varying biological fractionation or variable organic sourcing, as evidenced by the difference in stratigraphic expression in $\delta^{13}C_{org}$ relative to $\delta^{13}C_{carb}$ (Fig. 6). The magnitude of the Guttenberg excursion in $\delta^{13}C_{org}$ is *ca* 2‰, while the $\delta^{13}C_{carb}$ excursion is *ca* 2·5‰ at both locations. Other reported Guttenberg excursion $\delta^{13}C_{org}$ excursions were found to have magnitudes of *ca* 1‰ from West Virginia (Young *et al.*, 2008), *ca* 3‰ from Pennsylvania (Patzkowsky *et al.*, 1997) and *ca* 8‰ from Iowa (Pancost *et al.*, 1999). In this latter case, compound-specific analysis of TOC components was used to correct for organic matter source mixing; the resulting reconstructed, source-independent magnitude of the Guttenberg excursion was *ca* 3·5‰ (Pancost *et al.*, 1999). The $\delta^{13}C_{org}$ is particularly variable in the zone above and below the Millbrig at Highway MM and New London making exact correlations difficult and the absence of the Millbrig in the Iowa core makes comparison speculative. Higher order trends in $\delta^{13}C_{org}$ are apparent at Highway MM, which may result from source mixing (Pancost *et al.*, 1999), unidentified diagenesis, a complex local signal, and/or decoupling of the $\delta^{13}C_{org}$ and $\delta^{13}C_{carb}$ system.

During catagenesis (i.e. thermal cracking), TOC decreases as organic matter is converted to simple hydrocarbons (for example, methane). These resulting hydrocarbons are often depleted in ^{13}C, leaving the residual TOC enriched in ^{13}C. Similar trends can be obtained by biological remineralization of organic matter by microbial respiration during or after deposition. As such, cross-plots of $\delta^{13}C_{org}$ versus TOC can provide insight into processes that alter $\delta^{13}C_{org}$. A pattern of increasing $\delta^{13}C_{org}$ as TOC decreases can thus be indicative of alteration in the $\delta^{13}C_{org}$ signal (e.g. Dehler *et al.*, 2005) or mixture of isotopically distinct components (e.g. Johnston *et al.*, 2012). Instead, a trend toward low $\delta^{13}C_{org}$ with low TOC (this is particularly noticeable at New London) is observed; however, because the low TOC and ^{13}C-depleted samples come from strata below and above the Guttenberg excursion (Plattin and Kimmswick Limestones, respectively), while the high TOC, ^{13}C-enriched samples come from strata containing the Guttenberg excursion, this pattern most likely reflects primary environmental variability rather than alteration or contamination.

Nearly all autochthonous marine organic carbon is originally derived from the marine inorganic carbon reservoir by way of photosynthesis. Assuming a constant fractionation factor during photosynthesis, $\delta^{13}C_{org}$ should be consistently offset from $\delta^{13}C_{carb}$ by a fixed amount. This means that $\delta^{13}C_{carb}$ and $\delta^{13}C_{org}$ should move in parallel. The isotopic offset between coeval carbonate and organic carbon, $\Delta^{13}C$ ($=\delta^{13}C_{carb} - \delta^{13}C_{org}$), can be plotted to visually show if either carbon profile deviates from parallel behaviour. The $\Delta^{13}C$ profiles (Fig. 6) are similar between sections only from the HMKL-1/NLKL-1 bentonites on the rising limb of the Guttenberg excursion to the excursion termination. The $\Delta^{13}C$ curves from Highway MM and New London have a similar morphology to the $\Delta^{13}C$ curves from Iowa and Pennsylvania (Patzkowsky *et al.*, 1997) in that all curves immediately decline following peak-Guttenberg excursion values. This is evidence of a spatially coherent $\Delta^{13}C$ signal (on at least the continental-scale) with varying degrees of local overprinting. The authors agree with Pancost *et al.* (1999), who argued that $\delta^{13}C_{org}$ correlations during this interval will be complicated by source mixing and prefer to use (screened and filtered) $\delta^{13}C_{carb}$, rather than $\delta^{13}C_{org}$ for continental and global correlations. Excluding the Decorah Formation, the lack of strong agreement in $\Delta^{13}C$ between sections suggests that existing paired $\delta^{13}C_{carb}$ and $\delta^{13}C_{org}$ data are insufficient to answer questions of global biogeochemical C cycling patterns across the whole study interval. More data, reflecting regionally reproducible trends, will be needed to extract additional meaning and evaluate possible causes of $\Delta^{13}C$ variation.

Correlation summary

The Guttenberg excursion is a clearly identifiable chemostratigraphic feature in both sections presented here regardless of the degree of sample screening and filtering. Correlations with unprocessed data have higher scatter (Fig. 6) and as such, the unprocessed signal has less potential to make the confident high-resolution correlations needed to test geochemically based hypotheses. For example, a compilation of all data from this work (i.e. including those that did not pass the screening or filtering) would result in a Guttenberg excursion morphology that is relatively depleted in ^{13}C and more similar to that of the $\delta^{13}C_{carb}$ profile from Eureka, Missouri, a location *ca* 13 km from Highway MM (Ludvigson *et al.*, 1996). It is possible that differences between the 'least-altered' data and

the adjacent $\delta^{13}C_{carb}$ profile from Eureka could arise from local water column gradients; however, based on both the scatter in the unscreened data and the similarity between the two 'least-altered' $\delta^{13}C_{carb}$ profiles, it seems mechanistically more plausible that the lower $\delta^{13}C$ values and stratigraphic variability of the Eureka section (Ludvigson *et al.*, 1996) may in part arise from sample selection, insufficient sampling density and/or diagenetic overprinting rather than the preservation of a primary $\delta^{13}C_{carb}$ signature. Detailed analysis of isotopic variability – in the context of petrographic and geochemical indicators for alteration – is necessary to ascertain the origin of these disparities. High-resolution correlations using processed data (Fig. 11) show that carefully screened bulk $\delta^{13}C_{carb}$ data can be used to correlate sections that at first glance seem to have significant local overprints, a problem that has hindered high-resolution correlations across Late Ordovician Laurentia (e.g. Ludvigson *et al.*, 2004; Young *et al.*, 2005; Bergström *et al.*, 2010a,b; Coates *et al.*, 2010). While it may not be required for lower-order correlations, detailed sample screening can greatly increase knowledge of the sources of $\delta^{13}C_{carb}$ variability and fine-tune the understanding of basin-scale sedimentary and geochemical processes.

Depositional facies, sea-level, $\delta^{13}C$ and $\delta^{18}O$

Facies likely exhibited both direct and indirect controls on $\delta^{13}C_{carb}$ and $\delta^{18}O_{carb}$ values at the bed scale and formation scale. Single beds (i.e. hand samples) showed differing isotope values related to burrow abundance and grain size. For example, samples from the peritidal Plattin Limestone contained high amounts of calcitic mud with relatively invariant $\delta^{13}C_{carb}$ and $\delta^{18}O_{carb}$ values, while burrows were isotopically more variable. The burrows likely functioned as conduits for post-depositional fluids and represent an indirect control of facies on isotope values. Samples from more hydrologically energetic facies, such as the Kimmswick Limestone, contained exhumed clasts from underlying formations, a direct control on bulk isotope values. Grainstones also are more porous than mudstones, facilitating inclusion of primary cements (direct control) and later recrystallization (indirect control). The more energetic facies limit the amount of carbonate mud, requiring sampling of the clast-cement mixtures that are associated with lower $\delta^{13}C_{carb}$ and $\delta^{18}O_{carb}$ values. In this context grainstone facies are more susceptible to alteration (and an apparent isotopic offset) than muddier lithologies from less energetic facies. This seems to be the most likely cause for the low $\delta^{18}O_{carb}$ values in the grainstones of the Glencoe Shale and Kimmswick Limestone relative to the Decorah Formation and Plattin Limestone.

Facies controls on isotope values at the formation scale include the biological pump (Freeman, 2001) and 'aquafacies' model (*sensu* Holmden *et al.*, 1998) and are the result of sea-level, microbial activity and connectivity with the open ocean. As a result of the biological pump, DIC in shallow waters will become relatively enriched in ^{13}C as ^{12}C-rich organic carbon is formed and subsequently exported to the deep ocean (where part of it may be oxidized back to DIC). In contrast, the aquafacies model invokes local oxidation of organic matter to generate shallow waters of the cratonic interior that are hydrologically restricted and depleted in ^{13}C relative to the open ocean. These models can be compared with $\delta^{13}C_{carb}$ values observed for Localities Highway MM and New London. The highest $\delta^{13}C_{carb}$ values were observed in the Kings Lake and Guttenberg Formations, both of which are thought to represent the deepest and lowest energy facies. This result is opposite of what the biological pump model predicts and suggests that the biological pump is not controlling the stratigraphic variation in $\delta^{13}C_{carb}$ values in this interval in the Missouri area. The peak Guttenberg excursion values observed here match those in other Laurentian localities and do not match predicted $\delta^{13}C_{carb}$ for the Missouri region based on aquafacies-induced gradients in $\delta^{13}C_{DIC}$ (Young *et al.*, 2005). This suggests that the aquafacies model is not appropriate for this interval at these locations.

Isotope gradients can also result from more localized phenomena. Previous work on a slope to platform top transect of Carboniferous carbonates from north-west Spain (Immenhauser *et al.*, 2003) revealed a $\delta^{13}C_{carb}$ gradient with heaviest values occurring in the deepest facies. Immenhauser *et al.*, 2003 explain the heavier $\delta^{13}C_{carb}$ values as resulting from the increased proportion of ^{13}C-enriched ocean water mixed in during high-amplitude transgression and varying early diagenetic histories. A proportionally lower amount of ^{13}C-enriched waters is mixed with the 'aged' platform top water in offshore areas resulting in a relatively lower $\delta^{13}C_{carb}$ profile in the more shoreward facies. This mixing model is also not

appropriate for the Guttenberg excursion for several reasons. First, this excursion is confidently correlated over multiple basins on the Laurentian craton and believed to be a global event, which is not the case for the middle Atokan $\delta^{13}C_{carb}$ shift (Immenhauser *et al.*, 2003). This suggests that the mechanism responsible for the Guttenberg excursion would have to apply to the entire craton, if not the globe, and therefore includes numerous different facies and at a spatial scale where it is unrealistic to expect riverine waters to significantly impact $\delta^{13}C_{carb}$. Second, if the Guttenberg excursion represents the simple mixing of ocean water with ^{13}C-depleted, chemically-evolved epeiric platform water then the open ocean baseline must have been +3‰. (The absence of any abyssal Ordovician-aged sea floor precludes establishing an independent open ocean baseline.) If so, then the entire suite of existing records for this geological period does not preserve an open ocean signal (e.g. Bergström *et al.*, 2009b). Finally, while sea-level is thought to have risen throughout the Late Ordovician (Munnecke *et al.*, 2010), there is no corresponding, continuous increase in $\delta^{13}C_{carb}$ of epeiric carbonates associated with this increase in ocean connectivity. Therefore, it does not appear that a transgression that increased ocean connectivity everywhere was the responsible for the Guttenberg excursion.

Another model explaining the relation between sea-level and $\delta^{13}C_{carb}$ has been proposed by Fanton & Holmden (2007), whereby sea-level rise was accompanied by an increased flux of nutrient-rich open ocean water to the inner craton. This led to locally increased primary productivity and organic carbon burial, which in turn increased $\delta^{13}C_{DIC}$. However, the agreement in $\delta^{13}C_{carb}$ values during the Guttenberg excursion across the Laurentian palaeocontinent argues that the origin of the higher $\delta^{13}C_{carb}$ values is the result of *global* processes (for example, global organic carbon burial) rather than local or regional processes (for example, runoff contributions from nearby highlands, microbial oxidation of organic matter).

Regional and global implications

Correlations from screened and filtered data give insight into the geochemical nature of ancient epeiric seas by discriminating against secondary signals. The correlations between New London and Highway MM are consistent with the Guttenberg excursion being an isochronous excursion that occurred in an isotopically well-mixed ocean. The magnitude of the Guttenberg excursion reported here (2·5‰) is comparable to those reported for the Guttenberg excursion from Iowa (2‰, Pancost *et al.*, 1999; 1·5 to 3‰, Ludvigson *et al.*, 2004), Pennsylvania (3‰, Patzkowsky *et al.*, 1997), Kentucky (2·0‰, Coates *et al.*, 2010), Virginia (2‰, Young *et al.*, 2005), West Virginia (2‰, Young *et al.*, 2005) and Tennessee (2·0 to 2·5‰, Bergström *et al.*, 2010a) (Fig. 12). The pre-excursion, peak-excursion and post-excursion values reported here also very closely match those reported for the 'generalized $\delta^{13}C_{carb}$ curve' of Bergström *et al.* (2009b) (Fig. 12). Compilation of these data can be used to understand geographic gradients and stratigraphic variability in $\delta^{13}C_{carb}$ records and their possible syndepositional and diagenetic causes.

Despite the general agreement in the aforementioned Guttenberg excursion $\delta^{13}C$ records, a detailed examination of some reports reveals local and regional variations in the stratigraphic expression of the Guttenberg excursion. For a single location in eastern Iowa, Ludvigson *et al.* (1996) argued that primary micritic $\delta^{13}C_{carb}$ might be decoupled from coeval brachiopod $\delta^{13}C_{carb}$ signatures as a result of water column stratification. Comparisons of bulk carbonate $\delta^{13}C_{carb}$ data with coeval brachiopods from St. Louis County, Missouri (Shields *et al.*, 2003) show no systematic difference between the two material types, although the stratigraphic resolution of the brachiopods is low and the scatter in $\delta^{13}C_{carb}$ is relatively high in the Castlewood Limestone and Glencoe Shale equivalents, where the brachiopods were sampled. The present authors find no evidence for the stratification of the inner cratonic sea in the Missouri region.

Laterally restricted aquafacies with unique water column isotopic signatures have been proposed as an explanation for regional patterns in $\delta^{13}C_{carb}$ during the Guttenberg excursion (e.g. Young *et al.*, 2005). The data set of Ludvigson *et al.* (2004) shows apparent spatial variability in Guttenberg excursion $\delta^{13}C_{carb}$ curves in six cores from Iowa. Localites 4 and 5 of Ludvigson *et al.*, 2004 have a $\delta^{13}C_{carb}$ profile very similar to that of New London while Locality 1 (located <50 km away from Localities 4 and 5) shows a different morphology; cores farther away have even more divergent profiles (Fig. 12B). It is possible that these cores reflect different water column processes on the regional scale. Yet, the presence of Guttenberg excursion curves in Iowa

that have the same pre-excursion, peak-excursion and post-excursion values as the Missouri sections presented in this work (Fig. 12B) and from more distal locations (for example, West Virginia) (Fig. 12C) suggests an alternative explanation, namely: *local syndepositional and post-depositional alteration is superimposed over a signal representing precipitation from an isotopically homogenous epeiric sea*. A prevalent mechanism by which such local variation could result is the metabolic oxidation of organic matter by microbes, which has been proposed as a contributing factor producing lower $\delta^{13}C_{carb}$ values in the pore waters and modern sediments of the Bahama Banks and Florida (Patterson & Walter, 1994). This results in scattered and lower average $\delta^{13}C_{carb}$ values on the local scale. The present authors find this explanation more consistent with the data from this report than stratigraphically coherent gradients in $\delta^{13}C_{DIC}$ in the ancient ocean, which should not produce the observed $\delta^{13}C_{carb}$ trends characterized by high scatter and low $\delta^{13}C_{carb}$ values. The Iowa cores with $\delta^{13}C_{carb}$ profiles similar to the two new Missouri sections (despite the >1000 km distance between the Iowa and Missouri sections and the open ocean) may be the most representative of open marine values, whereas the stratigraphically variable $\delta^{13}C_{carb}$ profiles in adjacent cores (despite their proximity to each other) would result from diagenetic alteration or a local water-column signal that is unrelated to any large-scale 'ocean-to-inner craton' gradient. Importantly, the sections with low stratigraphic scatter in $\delta^{13}C_{carb}$ all meet the 'generalized' peak-Guttenberg excursion value (*ca* 2·5‰) of Bergström *et al.* (2009b), while sections with higher scatter do not meet the peak value. The $\delta^{13}C_{carb}$ scatter is preferentially toward lower $\delta^{13}C_{carb}$ values. This differs from true 'noise' (i.e. random scatter around a mean value), which should also have values that are *heavier* than the mean $\delta^{13}C_{carb}$, which is not observed (Fig. 12B and C). In this view, the midcontinent Guttenberg excursion curve (corresponding to 'midcontinent aquafacies') of Young *et al.* (2005) was constructed using sections that may have been impacted by diagenetic overprinting and does not reflect a primary craton-scale $\delta^{13}C_{carb}$ gradient. This interpretation suggests that more locations may have undergone more substantial diagenetic alteration than previously assumed.

This work does not argue that large-scale isotopic gradients could not exist in another time period or location, or for isotopic systems other than carbon (for example, neodymium). This work does argue that for the specific case of midcontinent records of the Guttenberg excursion no long-range spatial gradient in $\delta^{13}C_{carb}$ is required to explain the observed trends. Instead, the existing Guttenberg excursion records are more parsimoniously interpreted as reflecting differential alteration of a spatially *homogenous* primary $\delta^{13}C_{carb}$ signal, rather than faithful preservation of what is essentially a spatially *heterogenous* $\delta^{13}C_{carb}$ primary signal. Figure 12B separates the midcontinent aquafacies into two categories, those thought to track the global $\delta^{13}C_{carb}$ record and those that do not, the former being suitable for chemostratigraphic correlation and reconstructions of ocean chemistry. Missouri sections Highway MM and New London (Midcontinent aquafacies) have the same basic Guttenberg excursion values as the more hydrologically connected Taconic and Southern aquafacies sections. Correlation with Iowa sections suggests that any pre-existing regional $\delta^{13}C_{carb}$ gradient (Panchuk *et al.*, 2006) was abolished in the Missouri-Iowa region during Guttenberg excursion-time coincident with the craton-wide Mohawkian transgression (e.g. Kolata *et al.*, 1998, 2001).

It is clear that studies used to reconstruct spatial or temporal variability in ocean chemistry or carbon cycling need to be conducted at a high sampling resolution and data need to be placed in a rigorous depositional context and evaluated based on petrographic and geochemical indicators of alteration whenever possible. Because the understanding of oceanic connectivity and the biogeochemical C-cycle hinge on $\delta^{13}C_{carb}$ chemostratigraphic correlations, differing treatment of data sets can profoundly change the understanding of the Earth System.

CONCLUSIONS

This work supplies techniques for assessing diagenetic alteration of $\delta^{13}C_{carb}$ and $\delta^{18}O_{carb}$ over a large range of spatial scales and contributes to the general understanding of carbon-isotope homogeneity and hydrological connectivity in ancient epeiric seas. Results from this work demonstrate that the variable Guttenberg carbon isotope excursion profiles can be explained in terms of local diagenetic alteration and are not consistent with the previously proposed 'aquafa-

cies' model, which invoked an isotopically heterogeneous epeiric sea that formed as a result of a stable long-term and long-range ocean to craton $\delta^{13}C_{DIC}$ gradient. Specifically:

1 Significant isotopic heterogeneity (up to 2‰ in $\delta^{13}C_{carb}$ and 3‰ in $\delta^{18}O_{carb}$) within single hand samples can be superimposed over the Guttenberg carbon isotope excursion. These variations typically result from the admixture of multiple isotopically distinct components of primary and secondary origin, rather than from dynamic carbon cycling or spatially heterogeneous reservoirs. Screening of $\delta^{13}C_{carb}$ data using petrographic, geochemical and isotopic methods explains apparent differences in $\delta^{13}C_{carb}$ profiles between sections and the resulting correlations have higher stratigraphic resolving power than unprocessed data.

2 Normalized $\delta^{13}C_{carb}$ excursion profiles can help identify alteration at the outcrop scale by comparing $\delta^{13}C_{carb}$ morphologies from within a single basin. Normalized $\delta^{13}C_{carb}$ curves for the Guttenberg excursion show that ^{13}C-enriched locations have regionally reproducible $\delta^{13}C_{carb}$ profiles and low $\delta^{13}C_{carb}$ scatter. In contrast, sections that are relatively depleted in ^{13}C are associated with poor regional reproducibility of $\delta^{13}C_{carb}$ trends and high $\delta^{13}C_{carb}$ scatter, patterns consistent with local diagenetic alteration.

3 The strong agreement in absolute values of $\delta^{13}C_{carb}$ before, at the peak of, and after the Guttenberg excursion in sections identified as 'least-altered' support an isotopically homogenous carbon reservoir.

4 Paired $\delta^{13}C_{carb}$ and $\delta^{13}C_{org}$ data yield $\Delta^{13}C$ profiles that are similar during the peak and falling stage of the Guttenberg excursion; the regional reproducibility of this trend suggests preservation of a primary $\Delta^{13}C$ signature in this interval with possible global implications.

Chemostratigraphic correlations between Localities Highway MM and New London give insight into the temporal and spatial relations of Upper Ordovician strata in central and northern Missouri and relate them to other strata of similar age.

1 High-resolution $\delta^{13}C_{carb}$ records show that the Upper Kings Lake and Guttenberg Limestones in Missouri, previously thought to be successive, are largely coeval. The stratigraphically smooth $\delta^{13}C_{carb}$ profiles support a less substantial erosional history in eastern Missouri during post-Kings Lake, pre-Kimmswick time than has been previously reported.

2 Lithological and chemostratigraphic evidence suggests that a thickening of the Guttenberg excursion interval in northern Missouri largely resulted from an increased relative sedimentation rate in northern Missouri during the last half of the Guttenberg excursion.

ACKNOWLEDGEMENTS

The authors wish to thank R. Folkerts for her indispensable assistance in the field; D. Kolata for guidance in the field and for discussions of the regional stratigraphy; D. McCay for help preparing and analysing samples; S. Young, R. Criss, F. Moynier and J. Catalano for discussions; P. Skemer for use of laboratory equipment; and B. Mahan for assistance with microscopy and photography. The manuscript was greatly improved by insightful comments from L. Kump and an anonymous reviewer as well as A. Immenhauser and T. Frank. Support was provided in part by funding from the Agouron Institute, the ACS Petroleum Research Fund (Grant No. 51357-DNI2), and a Hanse-wissenschaftskolleg Fellowship awarded to DAF. In addition, isotope analyses and travel were partly funded by a DOSECC graduate research grant and a GSA graduate research grant awarded to JGM.

REFERENCES

Allan, J.R. and **Matthews, R.K.** (1982) Isotope signatures associated with early meteoric diagenesis. *Sedimentology*, **29**, 797–817.

Bergström, S.M., **Agematsu, S.** and **Schmitz, B.** (2010c) Global Upper Ordovician correlation by means of $\delta^{13}C$ chemostratigraphy: implications of the discovery of the Guttenberg $\delta^{13}C$ excursion (Guttenberg excursion) in Malaysia. *Geol. Mag.*, **147**, 641–651.

Bergström, S.M., **Huff, W.D.**, **Saltzman, M.R.**, **Kolata, D.R.** and **Leslie, S.A.** (2004) The greatest volcanic ash falls in the Phanerozoic: Trans-Atlantic relations of the Ordovician Millbrig and Kinnekulle K-bentonites. *Sed. Rec.*, **2**, 4–8.

Bergström, S.M., **Xu, C.**, **Schmitz, B.**, **Young, S.**, **Jia-Yu, R.** and **Saltzman, M.R.** (2009a) First documentation of the Ordovician Guttenberg $\delta^{13}C$ excursion (Guttenberg excursion) in Asia: chemostratigraphy of the Pagoda and Yanwashan formations in southeastern China. *Geol. Mag.*, **146**, 1–11.

Bergström, S.M., **Chen, X.**, **Gutiérrez-Marco, J.C.** and **Dronov, A.** (2009b) The new chronostratigraphic classification of the Ordovician System and its relations to major regional series and stages and to δ13C chemostratigraphy. *Lethaia*, **42**, 97–107.

Bergström, S.M., **Schmitz, B.**, **Saltzman, M.R.** and **Huff, W.D.** (2010a) The Upper Ordovician Guttenburg δ13C excursion (Guttenberg excursion) in North America and Baltoscandia: occurrence, chronostratigraphic significance, and paleoenvironmental relationships. In: *Geol. Soc. Am. Spec. Pap.* (Eds S.C. Finney and W.B.N. Berry), **466** pp. 36–67.

Bergström, S.M., **Young, S.** and **Schmitz, B.** (2010b) Katian (Upper Ordovician) $\delta^{13}C$ chemostratigraphy and sequence stratigraphy in the United States and Baltoscandia: a regional comparison. *Palaeogeogr. Palaeoclimatol. Palaeoecol.*, **296**, 217–234.

Brand, U. (2004) Carbon, oxygen and strontium isotopes in Paleozoic carbonate components: an evaluation of original seawater-chemistry proxies. *Chem. Geol.*, **204**, 23–44.

Brand, U., **Tazawa, J.**, **Sano, H.**, **Azmy, K.** and **Lee, X.** (2009) Is mid-late Paleozoic ocean-water chemistry coupled with epeiric seawater isotope records? *Geology*, **37**, 823–826.

Brett, C.E., **McLaughlin, P.I.**, **Cornell, S.R.** and **Baird, G.C.** (2004) Comparative sequence stratigraphy of two classic Upper Ordovician successions, Trenton Shelf (New York-Ontario) and Lexington Platform (Kentucky-Ohio): implications for eustasy and local tectonism in eastern Laurentia. *Palaeogeogr. Palaeoclimatol. Palaeoecol.*, **210**, 295–329.

Coates, J.W., **Ettensohn, F.R.** and **Rowe, H.D.** (2010) Correlations across a facies mosaic within the Lexington Limestone of central Kentucky, USA, using whole-rock stable isotope compositions. In: *The Ordovician Earth System* (Eds S.C. Finney and W.B.N. Berry), *Geol. Soc. Am. Spec. Pap.*, **466** pp. 177–193.

Dehler, C.M., **Elrick, M.**, **Bloch, J.D.**, **Crossey, L.J.**, **Karlstrom, K.E.** and **Des Marais, D.J.** (2005) High-resolution delta C-13 stratigraphy of the Chuar Group (ca. 770–742 Ma), Grand Canyon: implications for mid-Neoproterozoic climate change. *Geol. Soc. Am. Bull.*, **117**, 32–45.

Epstein, S. and **Mayeda, T.K.** (1953) Variations of O^{18} content of waters from natural sources. *Geochim. Cosmochim. Acta*, **4**, 213–224.

Fanton, K.C. and **Holmden, C.** (2007) Sea-level forcing of carbon isotope excursions in epeiric seas: implications for chemostratigraphy. *Can. J. Earth Sci.*, **44**, 807–818.

Flügel, E. (2009) *Microfacies of Carbonate Rocks: Analysis, Interpretation and Application*. Springer Verlag, Berlin, 984 pp.

Freeman, K.H. (2001) Isotope Biogeochemistry of Marine Organic Carbon. In: *Reviews in Mineralogy & Geochemistry 43: Stable Isotope Geochemistry* (Eds J.W. Valley and D.R. Cole), **43**, 579–605. Mineralogical Society of America and Geochemical Society, Washington, DC.

Hayes, J.M., **Strauss, H.** and **Kaufman, A.J.** (1999) The abundance of ^{13}C in marine organic matter and isotopic fractionation in the global biogeochemical cycle of carbon during the past 800 Ma. *Chem. Geol.*, **161**, 103–125.

Holland, S.M. and **Patzkowsky, M.E.** (1997) Distal orogenic effects on peripheral bulge sedimentation: Middle and Upper Ordovician of the Nashville Dome. *J. Sed. Res.*, **67**, 250–263.

Holland, S.M. and **Patzkowsky, M.E.** (1998) Sequence stratigraphy and relative sea-level history of the Middle and Upper Ordovician of the Nashville Dome, Tennessee. *J. Sed. Res.*, **68**, 684–699.

Holmden, C., **Creaser, R.A.**, **Muehlenbachs, K.**, **Leslie, S.A.** and **Bergstrom, S.M.** (1998) Isotopic evidence for geochemical decoupling between ancient epeiric seas and bordering oceans: implications for secular curves. *Geology*, **26**, 567–570.

Huff, W.D. (2008) Ordovician K-bentonites: issues in interpreting and correlating ancient tephras. *Quatern. Int.*, **178**, 276–287.

Immenhauser, A., **Kenter, J.A.M.**, **Ganssen, G.**, **Bahamonde, J.R.**, **Vliet, A.V.** and **Saher, M.H.** (2002) Origin and significance of isotope shifts in Pennsylvanian carbonates (Asturias, NW Spain). *J. Sed. Res.*, **72**, 82–94.

Immenhauser, A., **Della Porta, G.**, **Kenter, J.A.M.** and **Bahamonde, J.R.** (2003) An alternative model for positive shifts in shallow-marine carbonate $\delta^{13}C$ and $\delta^{18}O$. *Sedimentology*, **50**, 953–959.

Immenhauser, A., **Holmden, C.** and **Patterson, W.** (2008) Interpreting the carbon-isotope record of ancient shallow epeiric seas: lessons from the recent. In: *Dynamics of Epeiric Seas* (Eds B.R., Pratt, B.R., Holmden), *Geol. Assoc. Can. Spec. Pap.*, **48**, 137–174.

Joachimski, M.M. (1994) Subaerial exposure and deposition of shallowing upward sequences: evidence from stable isotopes of Purbeckian peritidal carbonates (basal Cretaceous), Swiss and French Jura Mountains. *Sedimentology*, **41**, 805–824.

Johnston, D.T., **Macdonald, F.A.**, **Gill, B.C.**, **Hoffman, P.F.** and **Schrag, D.P.** (2012) Uncovering the Neoproterozoic carbon cycle. *Nature*, **483**, 320–324.

Jones, D.S., **Fike, D.A.**, **Finnegan, S.**, **Fischer, W.W.**, **Schrag, D.P.** and **McCay, D.** (2011) Terminal Ordovician carbon isotope stratiraphy and glacioeustatic sea-level change across Anticost Island (Québec, Canada). *Geol. Soc. Am. Bull.*, **123**, 1645–1664.

Kaljo, D., **Martma, T.** and **Saadre, T.** (2007) Post-Hunnebergian Ordovician carbon isotope trend in Baltoscandia, its environmental implications and some similarities with that of Nevada. *Palaeogeogr. Palaeoclimatol. Palaeoecol.*, **245**, 138–155.

Kay, G.M. (1935) Ordovician System of the upper Mississippi Valley. In: *Kansas Geological Society 9th regional field conference, Upper Mississippi River Valley*, (Ed. A.C. Trowbridge), pp. 281–295. Kansas Geological Society, Lawrence, KS.

Knoll, A.H., **Hayes, J.M.**, **Kaufman, A.J.**, **Swett, K.** and **Lambert, I.B.** (1986) Secular variation in carbon isotope ratios from Upper Proterozoic Successions of Svalbard and East Greenland. *Nature*, **321**, 832–838.

Kolata, D.R., **Frost, J.K.** and **Huff, W.D.** (1986) K-bentonites of the Ordovician Decorah Subgroup, upper Mississippi Valley: correlation by chemical fingerprinting. *Illinois State Geol. Surv. Circular*, **537**, 30.

Kolata, D.R., **Frost, J.K.** and **Huff, W.D.** (1987) Chemical correlation of K-bentonite bed in the Middle Ordovician Decorah Subgroup, upper Mississippi Valley. *Geology*, **15**, 208–211.

Kolata, D.R., **Huff, W.D.** and **Bergström, S.M.** (1996) Ordovician K-bentonites of eastern North America. *Geol. Soc. Am. Spec. Pap.*, **313**, 84.

Kolata, D.R., **Huff, W.D.** and **Bergström, S.M.** (1998) Nature and regional significance of unconformities associated with the Middle Ordovician Hagan K-bentonite complex in the North American midcontinent. *Geol. Soc. Am. Bull.*, **110**, 723–739.

Kolata, D.R., **Huff, W.D.** and **Bergström, S.M.** (2001) The Ordovician Sebree Trough: an oceanic passage to the Midcontinent United States. *Geol. Soc. Am. Bull.*, **113**, 1067–1078.

Kump, L. R. and **Arthur, M.A.** (1999) Interpreting carbon-isotope excursions: carbonates and organic matter. *Chem. Geol.*, **161**, 181–198.

Leslie, S.A. (2000) Mohawkian (Upper Ordovician) conodonts of eastern North America and Baltoscandia. *J. Paleontol.*, **74**, 1122–1147.

Leslie, S.A. and **Bergström, S.M.** (1997) Use of K-bentonite beds as time-planes for high-resolution lithofacies analysis and assessment of net rock accumulation rate: an example from the upper Middle Ordovician of eastern North America. In: *Paleozoic Sequence Stratigraphy, Biostratigraphy, and Biogeography: Studies in Honor of J. Granville ("Jess") Johnson* (Eds G. Klapper, M.A. Murphy, and J.A. Talent), *Geol. Soc. Am. Spec. Pap.*, **321**, 11–21.

Lohmann, K.C. (1988) Geochemical patterns of meteoric diagenetic systems and their application to studies of paleokarst. In: *Paleokarst* (Eds N.P. James and P.W. Choquette), pp. 416. Springer-Verlag, New York City.

Ludvigson, G.A., **Jacobson, S.R.**, **Witzke, B.J.** and **Gonzàlez, L.A.** (1996) Carbonate component chemostratigraphy and depositional history of the Ordovician Decorah Formation, Upper Mississippi Valley. In: *Paleozoic Sequence Stratigraphy; Views From the North American Craton* (Eds B.J. Witzke, G.A. Ludvigson and J. Day), *Geol. Soc. Am. Spec. Pap.*, **306**, 67–86.

Ludvigson, G.A., **Witzke, B.J.**, **Schneider, C.L.**, **Smith, E.A.**, **Emerson, N.R.**, **Carpenter, S.J.** and **González, L.A.** (2000) A profile of the mid-Caradoc (Ordovician) carbon isotope excursion at the McGregor Quarry, Clayton County, Iowa. *Geol. Soc. Iowa Guidebook*, **70**, 25–31.

Ludvigson, G.A., **Witzke, B.J.**, **Gonzàlez, L.A.**, **Carpenter, S.J.**, **Schneider, C.L.** and **Hasiuk, F.** (2004) Late Ordovician (Turinian-Chatfieldian) carbon isotope excursions and their stratigraphic and paleoceanographic significance. *Palaeogeogr. Palaeoclimatol. Palaeoecol.*, **210**, 187–214.

Martin, J.A., **Knight, R.D.** and **Hayes, W.C.** (1961) Ordovician System. In: *The Stratigraphic Succession in Missouri* (Ed. J.W. Koenig), *Missouri Geol. Surv. Water Resour.*, **40**, 32–35.

Martma, T. (2005) Ordovician carbon isotopes. In: *Estonian Geological Sections, Kerguta (564) Drill Core* (Ed. A. Põldvere), *Geol. Surv. Estonia Bull.*, **7**, 25–30.

McCracken, M.H. (1966) Major structural features of Missouri [Map]. Missouri Department of Natural Resources: Division of Geology and Land Survey, Rolla. http://www.dnr.mo.gov/geology/adm/publications/map-MajorStrucFeatures.pdf

McLaughlin, P.I. and **Brett, C.E.** (2007) Signatures of sea-level rise on the carbonate margin of a Late Ordovician foreland basin: a case study from the Cincinnati Arch, USA. *Palaios*, **22**, 245–267.

Missouri Department of Natural Resources (2009) *Generalized Geology Map of Missouri [Map]*. Missouri Department of Natural Resources: Division of Geology and Land Survey, Rolla. www.dnr.mo.gov/geology.

Mitchell, C.E., **Adhya, S.**, **Bergström, S.M.**, **Joy, M.P.** and **Delano, J.W.** (2004) Discovery of the Ordovician Millbrig K-bentonite Bed in the Trenton Group of New York State: implications for regional correlation and sequence stratigraphy in eastern North America. *Palaeogeogr. Palaeoclimatol. Palaeoecol.*, **210**, 331–346.

Munnecke, A., **Calner, M.**, **Harper, D.A.T.** and **Servais, T.** (2010) Ordovician and Silurian sea-water chemistry, sea level, and climate: a synopsis. *Palaeogeogr. Palaeoclimatol. Palaeoecol.*, **296**, 389–413.

Panchuk, K.M., **Holmden, C.** and **Kump, L.R.** (2005) Sensitivity of the epeiric sea carbon isotope record to local-scale carbon cycle processes: tales from the Mohawkian Sea. *Palaeogeogr. Palaeoclimatol. Palaeoecol.*, **228**, 320–337.

Panchuk, K.M., **Holmden, C.E.** and **Leslie, S.A.** (2006) Local controls on carbon cycling in the Ordovician midcontinent region of North America, with implications for carbon isotope secular curves. *J. Sed. Res.*, **76**, 200–211.

Pancost, R.D., **Freeman, K.H.** and **Patzkowsky, M.E.** (1999) Organic-matter source variation and the expression of a late Middle Ordovician carbon isotope excursion. *Geology*, **27**, 1015–1018.

Patterson, W.P. and **Walter, L.M.** (1994) Depletion of ^{13}C in seawater ΣCO_2 on modern carbonate platforms: significance for the carbon isotopic record of carbonates. *Geology*, **22**, 885–888.

Patzkowsky, M.E., **Slupik, L.M.**, **Arthur, M.A.**, **Pancost, R.D.** and **Freeman, K.H.** (1997) Late Middle Ordovician environmental change and extinction: Harbinger of the Late Ordovician or continuation of Cambrian patterns? *Geology*, **25**, 911–914.

Railsback, L.B., **Holland, S.M.**, **Hunter, D.M.**, **Jordan, E.M.**, **Díaz, J.R.** and **Crowe, D.E.** (2003) Controls on geochemical expression of subaerial exposure in Ordovician limestones from the Nashville Dome, Tennessee, U.S.A. *J. Sed. Res.*, **73**, 790–805.

Rodgers, J. (1971) The Taconic Orogeny. *Geol. Soc. Am. Bull.*, **82**, 1141–1178.

Scotese, C.R. and **McKerrow, W.S.** (Eds.) (1990) Revised world maps and introduction. In: *Paleozoic Paleogeography and Biogeography*, *Geol. Soc. London Mem.*, **12**, 1–21.

Sell, B.K. and **Samson, S.D.** (2011) Apatite phenocryst compositions demonstrate a miscorrelation between the Millbrig and Kinnekulle K-bentonites of North America and Scandinavia. *Geology*, **39**, 303–306.

Shields, G.A., **Carden, G.A.F.**, **Veizer, J.**, **Meidla, T.**, **Rong, J.Y.** and **Li, R.Y.** (2003) Sr, C, and O isotope geochemistry of Ordovician brachiopods: a major isotopic event around the Middle-Late Ordovician transition. *Geochim. Cosmochim. Acta*, **67**, 2005–2025.

Simo, J.A., **Emerson, N.R.**, **Byers, C.W.** and **Ludvigson, G.A.** (2003) Anatomy of an embayment in an Ordovician epeiric sea, Upper Mississippi Valley, USA. *Geology*, **31**, 545–548.

Swart, P.K. (2008) Global synchronous changes in the carbon isotopic composition of carbonate sediment unrelated to changes in the global carbon cycle. *Proc. Natl Acad. Sci. USA*, **105**, 13741–13745.

Templeton, J.S. and **Willman, H.B.** (1963) Champlainian Series (Middle Ordovician) in Illinois. *Illinois State Geol. Surv. Bull.*, **89**, 260.

Thompson, T.L. (1991) Paleozoic Successions in Missouri Part II: Ordovician System. *Missouri Geol. Surv. Rep. Invest.*, **70**, 110–213.

Tucker, R.D. (1992) U-Pb dating of plinian-eruption ashfalls by the isotope dilution method: a reliable and precise tool for time-scale calibration and biostratigraphic correlation. *Geol. Soc. Am. Meeting*, **24**, A198.

Tucker, R.D. and **McKerrow, W.S.** (1995) Early Paleozoic chronology: a review in light of new U-Pb zircon ages from Newfoundland and Britain. *Can. J. Earth Sci.*, **32**, 368–379.

Ulrch, E.O. (1904) The quarrying industry of Missouri. In: *Missouri Bureau of Geology and Mines Report* Vol. II, 2nd series (Eds E.R. Buckley and H.A. Buehler), **2**, pp. 109–111. Missouri Bureau of Geology and Mines, Jefferson City, MO.

Veizer, J., **Bruckschen, P.**, **Pawellek, F.**, **Diener, A.**, **Podlaha, O.G.**, **Carden, G.A.F.**, **Jasper, T.**, **Korte, C.**, **Strauss, H.**, **Azmy, K.** and **Ala, D.** (1997) Oxygen isotope evolution of Phanerozoic seawater. *Palaeogeogr. Palaeoclimatol. Palaeoecol.*, **132**, 159–172.

Veizer, J., **Ala, D.**, **Azmy, K.**, **Bruckschen, P.**, **Buhl, D.**, **Bruhn, F.**, **Carden, G.A.F.**, **Diener, A.**, **Ebneth, S.**, **Godderis, Y.**, **Jasper, T.**, **Korte, C.**, **Pawellek, F.**, **Podlaha, O.G.** and **Strauss, H.** (1999) $^{87}Sr/^{86}Sr$, $\delta^{13}C$ and $\delta^{18}O$ evolution of Phanerozoic seawater. *Chem. Geol.*, **161**, 59–88.

Witzke, B.J. and **Kolata, D.R.** (1988) Changing structural and depositional patterns, Ordovician Champlainian and Cincinnatian Series of Iowa-Illinois. *Iowa Dept. Nat. Resour. Guidebook*, **8**, 55–77.

Young, S.A., **Saltzman, M.R.** and **Bergström, S.M.** (2005) Upper Ordovician (Mohawkian) carbon isotope ($\delta^{13}C$) stratigraphy in eastern and central North America: regional expression of a perturbation of the global carbon cycle. *Palaeogeogr. Palaeoclimatol. Palaeoecol.*, **222**, 53–76.

Young, S.A., **Saltzman, M.R.**, **Bergstrom, S.M.**, **Leslie, S.A.** and **Xu, C.** (2008) Paired $\delta^{13}C_{carb}$ and $\delta^{13}C_{org}$ records of Upper Ordovician (Sandbian-Katian) carbonates in North America and China: implications for paleoceanographic change. *Palaeogeogr. Palaeoclimatol. Palaeoecol.*, **270**, 166–178.

Manuscript received 19 April 2012; revision accepted 16 January 2013

Supporting Information

Additional Supporting Information may be found in the online version of this article:

Table S1. Geochemical data for location New London.

Table S2. Geochemical data for location Highway MM. See Table S1 for column header definitions and stratigraphic abbreviations.

Table S3. $\delta^{18}O_{carb}$ filter table.